Formation and evolution of compact binaries in globular clusters: II. Binaries with neutron stars.

N. Ivanova [1]$\star$, C. Heinke[2]†, F. A. Rasio[2], K. Belczynski[3]‡, & J. Fregeau[2]

[1]*Canadian Institute for Theoretical Astrophysics, University of Toronto, 60 St. George, Toronto, ON M5S 3H8, Canada*
[2]*Northwestern University, Dept of Physics & Astronomy, 2145 Sheridan Rd, Evanston, IL 60208, USA*
[3]*New Mexico State University, Department of Astronomy, 1320 Frenger Mall, Las Cruces, New Mexico 88003-8001, USA*

29 June 2007

ABSTRACT

In this paper, the second of a series, we study the stellar dynamical and evolutionary processes leading to the formation of compact binaries containing neutron stars in dense globular clusters. For this study, 70 dense clusters were simulated independently, with a total stellar mass $\sim 2 \times 10^7 \, M_\odot$, well exceeding the mass of all dense globular clusters in our Galaxy. We find that, in order to reproduce the empirically derived formation rate of low-mass X-ray binaries (LMXBs), we must assume that NSs can be formed via electron-capture supernovae with typical natal kicks smaller than in core-collapse supernovae. Our results explain the observed dependence of the number of LMXBs on "collision number" as well as the large scatter observed between different globular clusters. We predict that the number of quiescent LMXBs should not have a strong metallicity dependence. For millisecond pulsars (MSPs), we distinguish high-magnetic-field (short-lived) and low-magnetic-field (long-lived) populations. With this distinction, we obtain good agreement of our models with the numbers and characteristics of observed MSPs in 47 Tuc and Terzan 5, as well as with the cumulative statistics for MSPs detected in globular clusters of different dynamical properties. We find that significant production of merging double neutron stars potentially detectable as short γ-ray bursts occurs only in very dense, most likely core-collapse clusters.

Key words: stellar dynamics – binaries: close – binaries: general – stars: neutron – pulsars: general – globular clusters: general – X-rays: binaries.

1 INTRODUCTION

Neutron stars (NSs) are seen in globular clusters (GCs) via their (current or past) participation in interacting binary systems. From the earliest observations of X-ray binaries in GCs it has been noted that their abundance per unit mass is $\sim$100 times greater in GCs than in the Galaxy as a whole (Clark 1975). This was understood to be a consequence of the high stellar density of GCs, which may lead to the creation of compact NS binaries in close stellar encounters. NS binaries are often relatively easy to identify in GCs (compared to other binaries), and they allow us to constrain the dynamical history of clusters and the evolution of NS properties in binary systems. They have been observed so far in three guises: (i) as bright low-mass X-ray binaries (LMXBs); (ii) as quiescent LMXBs (qLMXBs); and (iii) as binary or single millisecond pulsars (MSPs). In the future, they could also be detected as sources of gravitational radiation.

Bright LMXBs have X-ray luminosities of typically 10^{35}–10^{38} ergs s^{-1}. In bright LMXBs, the NS is actively accreting from a companion star via Roche-lobe overflow and an accretion disk. Thirteen sources are known in Galactic GCs, of which 12 are known to contain NSs through the detection of thermonuclear bursts. Six are transient systems (two have remained in outburst for more than a decade; the others have outburst time-scales of weeks), while the other seven seem to be persistent. Orbital periods have been identified for six systems (Dieball et al. 2005), of which half are below one hour, indicating an ultracompact system composed of a neutron star and white dwarf companion. Efficient surveys of the X-ray sky give us confidence that we have detected all bright LMXBs that have existed in Galactic GCs during the past 10 years.

Quiescent LMXBs have lower X-ray luminosities ($10^{31} < L_X < 10^{34}$ ergs/s), indicating that accretion is not active or is significantly reduced during quiescence. Their X-ray luminosity is thought to derive at least in part from the re-radiation of heat from the core of the NS, which was generated during accretion outbursts (Brown et al. 1998), though other mechanisms are also suggested (see, e.g., Campana et al. (1998)). They can be identified through their positional coincidence with the location of a bright transient LMXB in outburst (Wijnands et al. 2005), and/or through their characteristically soft X-ray spectrum (Rutledge et al. 2002).

[1] The total number of qLMXBs in the Galactic GC system is inferred to be ∼100-200 (Heinke et al. 2003), although only a fraction of the Galactic clusters have been studied sufficiently to identify qLMXBs.

As of this writing 129 millisecond radio pulsars have been observed in GCs, with more than 10, 20 and 30 seen from the clusters M28 (Stairs et al. 2006), 47 Tuc (Camilo et al. 2000), and Terzan 5 (Ransom et al. 2005), respectively [2]. These millisecond pulsars (MSPs) are thought to be descendants of LMXBs (e.g., Bhattacharya & van den Heuvel 1991). It is estimated that of order 1000 MSPs are present in the Galactic GC system (Heinke et al. 2005), of which half or more are potentially detectable. Current pulsar searches have reached the bottom of the pulsar luminosity function in very few clusters (e.g., 47 Tuc and M15). As an example, the total radio luminosity from Terzan 5 suggested that this cluster may contain 100 pulsars (Fruchter & Goss 1995)—this number is 3 times more than the number of identified pulsars.

Since NSs in GCs appear to be excellent tests for our understanding of both stellar dynamics and neutron star evolution, it is not surprising that this issue has attracted significant continuing attention. The largest challenge for these studies is computational. It has been estimated that a cluster consisting of 10^6 stars ($\sim 250,000 M_\odot$) will contain only a few hundred NSs, and models with a smaller number of stars will not therefore have sufficient statistics. Direct N-body methods are unlikely to address the million-body problem before 2020 (Hut 2006). Monte Carlo methods now allow million-body simulations for spherically symmetric systems with single stars (Giersz 2006) and with large fractions of primordial binaries, including direct integrations of all binary encounters (Fregeau & Rasio 2006), but a full implementation of binary star evolution is still lacking (Rasio et al. 2006). As a result, most previous theoretical studies of NSs in clusters were performed using simple scattering experiments, with a static background of single or binary stars (e.g., Sigurdsson & Phinney 1995; Rasio et al. 2000; Kuranov & Postnov 2006). We chose instead to use a method that treats in detail the stellar evolution of a large population of stars and binaries in a dense cluster environment, but with a highly simplified description of the stellar dynamics which is not fully self-consistent.

In this paper we present the results of our ongoing study of compact binary formation in GCs, concentrating on the formation of binaries with NSs. For the first time we have used cluster simulations that include a dynamically evolving system and represent consistently an entire stellar population with numbers of stars and binaries comparable to those in observed GCs. In addition, several statistically independent simulations were performed for each cluster model, to show how different the outcomes can be with slightly different but equivalent initial conditions. Some preliminary results on NS binaries from our work were reported in Ivanova & Rasio (2004); Ivanova et al. (2005); Ivanova & Rasio (2005); Rasio et al. (2006), and detailed results for the formation of binaries containing white dwarfs (WDs) were presented in Paper I (Ivanova et al. 2006). We refer the reader to Paper I for a complete description of the physical processes of formation and destruction of mass-transferring compact binaries, as well as our numerical methods. We outline updates to the method and our assumptions that are especially relevant to NSs in Section 2. In Section 3 we describe

the range of GC models that we consider. Formation and retention of NSs are analyzed in Section 4, and the following section is devoted to the formation of binaries containing NSs. We discuss the formation of LMXBs in Section 6, and MSPs are considered in Section 7. Section 8 briefly describes double neutron stars. We conclude by summarizing the connection between our results and the observations, as well as giving predictions for future observations and discussing constraints on NS formation.

2   METHOD

Our numerical methods generally remain the same as described in Ivanova et al. (2005, 2006). To study the population of NSs, we introduced a number of updates to the population synthesis model specifically for NS formation, and we revised the treatment of dynamical events with NSs. We also optimized numerical aspects of our code for more efficient use of parallel supercomputers.

2.1   Population synthesis updates

We adopt the binary evolution model from the population synthesis code `StarTrack` (Belczynski et al. 2002, 2007). In our first study of binary populations in GC cores (Ivanova et al. 2005) we used a previous version of `StarTrack` described in Belczynski et al. (2002). In our study of close binaries with white dwarfs (Ivanova et al. 2006, paper I) we employed a more recent version of `StarTrack` available at the time (as in Belczynski et al. 2007, but including updates only for WD evolution compared to the previous version). In this paper we incorporated all the latest updates of `StarTrack`, as described in Belczynski et al. (2007). Below we outline several of the most important changes in `StarTrack` that affect the formation and evolution of NSs compared to our previous studies of NSs in GCs (Ivanova & Rasio 2004; Ivanova et al. 2005, 2006). We also provide detailed descriptions of further modifications to the `StarTrack` model, beyond those in Belczynski et al. (2007), which we developed for the treatments of electron-capture supernovae and common-envelope events.

2.1.1   Natal kicks and supernova disruptions

At the moment of formation, both NSs and BHs receive additional speed (a natal kick), most likely due to asymmetric supernova ejecta (Fryer 2004). Although most recent simulations are in relatively good agreement with the measured distribution of pulsar velocities, the agreement is not yet firmly established (Scheck et al. 2006). In this paper we adopt the most recently derived pulsar kick velocity distribution from Hobbs et al. (2005), which is a Maxwellian distribution with one-dimensional RMS velocity $\sigma = 265$ km s^{-1} (the mean three-dimensional velocity is ~ 400 km s^{-1}). In contrast to some earlier studies (e.g., see Arzoumanian et al. 2002), no evidence for a bimodal velocity distribution is present.

At the moment of the explosion, the supernova progenitor can be a binary companion. Because of the kick, the binary can become unbound (and the binary components will separate) or the entire binary can be affected by the natal kick. In our previous studies, in order to find the velocities of the components of an unbound binary, we used the derivation by Tauris & Takens (1998), where the pre-supernova orbit is assumed to be circular. The approach used in the current version of `StarTrack` allows us to properly calculate

---

cases with an arbitrary pre-explosion orbital eccentricity (for full details, see §6.3 in Belczynski et al. 2007).

2.1.2 Electron-capture supernovae

Through our studies of accreting WDs (Ivanova et al. 2006) we found that electron-capture supernovae (ECSe) could be the dominant source of retained NSs in clusters. Similar results were also recently obtained in Kuranov & Postnov (2006). We have therefore considered in great detail all possible types of ECSe for this work.

It has been argued that when a *degenerate* ONeMg core reaches $M_{ecs} = 1.38 M_\odot$, its collapse is triggered by electron capture on ^{24}Mg and ^{20}Ne before neon and subsequent burnings start and, therefore, before the iron core formation (Miyaji et al. 1980; Nomoto 1984, 1987; Timmes & Woosley 1992; Timmes et al. 1994). The explosion energy of such an event is significantly lower than that inferred for core-collapse supernovae (Dessart et al. 2006). There are several possible situations when a star can develop a degenerate ONeMg core that will eventually reach M_{ecs}.

First, this can occur during the normal evolution of single stars. It was initially proposed by Barkat et al. (1974) that a star of 7–10 $M_\odot$, after non-explosive carbon burning, develops an ONeMg core. If the initial core mass is less than required for the neon ignition, $1.37 M_\odot$, the core becomes strongly degenerate. Through the continuing He shell burning, this core grows to M_{ecs}. In more massive stars, $\gtrsim 10\ M_\odot$, carbon, oxygen, neon and silicon burnings progress under non-degenerate conditions, and, in less massive stars, ONeMg cores never form. The formation of degenerate or non-degenerate ONeMg cores depends on the He core mass at the start of the asymptotic giant branch, where $\sim 2.5\ M_\odot$ is a rough boundary between the cases (Nomoto 1984). If the initial He core mass is below $1.83\ M_\odot$, no off-centre ignition will happen—the carbon core burning will occur when the degenerate core reaches the Chandrasekhar mass, resulting in a thermonuclear explosion (Hurley et al. 2000, also J. Eldridge 2006, priv. comm.).

The conditions for ECS were shown to occur in single stars of initial mass 8–10 $M_\odot$ by Nomoto (1984). This critical mass range depends on the properties of the He and CO cores, which, in turn, are highly dependent on the mixing prescription (semiconvection, overshooting, rotational mixing, etc.) as well as on the adopted opacities. As a result, the range varies between different evolutionary codes (see discussion in Podsiadlowski et al. 2004; Siess 2006), and is generally reduced compared to that proposed initially by Nomoto (1984, 1987). In the code that we use for our cluster simulations, a non-degenerate ONeMg core is formed when the initial He core mass is about 2.25 $M_\odot$ (Pols et al. 1998; Hurley et al. 2000) and the range of initial masses for single stars of solar metallicity that leads to the formation of such a core is 7.66 to 8.26 $M_\odot$. The equivalent mass ranges are from 6.85 to 7.57 $M_\odot$ and from 6.17 to 6.76 $M_\odot$ for single stars with GC-like metallicities, $Z = 0.005$ and $Z = 0.0005$, respectively.

The initial stellar mass is not the only parameter that defines whether a star will form a degenerate ONeMg core. It was recently pointed out by Podsiadlowski et al. (2004) that the range of progenitor masses for which an ECS can occur depends also on the mass transfer history of the star, and therefore may be different for binary stars, making it possible for more massive progenitors to collapse via ECS. We will refer to the single and binary scenarios for ECS in non-degenerate stars, as described above, as evolution-induced collapse (EIC).

The second possibility for an ECS to occur is by accretion on to a degenerate ONeMg WD in a binary: accretion-induced collapse (AIC). In this case, a massive ONeMg WD steadily accumulates mass until it reaches the critical mass M_{ecs} (for more detail on the adopted model of the accretion on the WD see Ivanova & Taam 2004; Belczynski et al. 2007). In addition, ONeMg WDs can be formed from CO WDs via off-centre carbon ignition if the mass of CO WDs is above 1.07 $M_\odot$ and the accretion rate is high, $\dot{M} > 2.7 \times 10^{-6} M_\odot \mathrm{yr}^{-1}$ (Kawai et al. 1987) so that eventually this also leads to AIC.

The third case that we consider is coalescing double WDs with a total mass exceeding M_{ecs}. To distinguish it from AIC, we will refer to this case as merger-induced collapse (MIC). The nature of NS formation is the same as in the case of AIC (accumulation of mass by a massive ONeMG WD). In the case of coalescing CO WDs, then, as in the case of single stars, off-centre carbon ignition occurs first, which quiescently converts the star into an ONeMg core, and this proceeds with an ECS (Saio & Nomoto 1985, 2004). Although the approach above was proposed for coalescing WDs in binaries only, we assume that in the case of *collisions* between two WDs it is applicable as well: except for the rare cases of near head-on collisions, a less massive WD will be tidally disrupted and accreted at high rate on to the more massive WD.

We therefore assume in our simulations that a NS will be formed via ECS in the following cases:

- if at the start of the AGB the He core mass is $1.83\ M_\odot \lesssim M_{c,BAGB} \lesssim 2.25\ M_\odot$ (EIC)
- if an accreting ONeMg WD reaches M_{ecs} (AIC)
- if the total mass of two merging or colliding WDs exceeds M_{ecs} (MIC)

For NSs formed via ECS we assume that the values of natal kick velocities are proportional to the explosion energies and, accordingly, are ten times smaller than in the core-collapse case (Dessart et al. 2006). We will provide the separate statistics for NSs created by different channels (core-collapse, EIC, AIC or MIC), so that if one of the channels later turns out to have been overestimated it will be easy to make the recalibration.

The gravitational mass of the newly formed NS is 1.26 $M_\odot$. This is ~ 0.9 of its baryonic mass (which cannot exceed the pre-collapse core mass) after subtracting the binding energy and is calculated as in Timmes et al. (1996):

$$M_{\mathrm{baryon}} - M_{\mathrm{grav}} = \Delta M = 0.075 M_{\mathrm{grav}}^2 \ , \tag{1}$$

where the masses are in solar masses. As the angular momentum of the binary is conserved, in the case of no kick, the binary widens.

The condition for ECS to occur depends essentially on the central density of the object. As a consequence, a rapidly rotating WD can reach a much higher mass than the Chandrasekhar limit before the central density becomes high enough for electron captures on ^{24}Mg and ^{20}Ne to occur. For example, its mass can be as high as 1.92 $M_\odot$ if the ratio of the WD rotational energy to the gravitational binding energy is 0.0833 and the star is highly oblate (Dessart et al. 2006). Such rapidly rotating heavy WDs can be formed, e.g., during the coalescence of two WDs with total mass exceeding the Chandrasekhar mass. During such a merger, less than 0.5 per cent of mass will be lost from the system (Guerrero et al. 2004). The collapse of a rapidly rotating WD can therefore lead to the formation of a more massive and very fast spinning NS.

2.1.3 Convective and radiative envelopes

The presence or absence of a deep outer convective envelope influences a star's behavior during various phases of close binary inter-

actions (e.g., angular momentum loss via magnetic braking, tidal interactions, stable or unstable mass transfer). In particular, it has been pointed out in Ivanova (2006) that the absence of a deep outer convective zone in low-metallicity GCs may explain the preferential formation of LMXBs in metal-rich clusters (Grindlay 1993; Bellazzini et al. 1995; Zepf et al. 2006).

In this study, for main-sequence stars we adopt the metallicity-dependent mass range to develop a convective envelope described by (eq.(10) in Belczynski et al. 2007) In addition, in our previous work, all giant-like stars were assumed to have outer convective envelopes. Now stars crossing the Hertzsprung gap and stars in the blue loop are not assumed to have convective envelopes if their effective temperature satisfies $\lg T_{\rm eff} > 3.73$.

2.1.4   Common-envelope phases

For common-envelope (CE) events we use the standard energy formalism (Webbink 1984). In this approach, the outcome of the CE phase depends on the adopted efficiency for orbital energy transfer into envelope expansion energy $\alpha_{\rm ce}$ and on the donor envelope central concentration parameter λ. The commonly used prescription is $\alpha_{\rm ce} \times \lambda = 1$, and this is adopted in our models as well. However, for He stars with an outer convective envelope we determine λ from the set of detailed He star evolution models calculated by Ivanova et al. (2003). In this case, $\lambda = 0.3R^{-0.8}$, where R is the radius of the He star in solar radii. As many He stars end their lives as NSs, the CE evolution of He stars is an important channel for the formation of close binaries with NSs. Indeed, the prescription above was recently used in a study of double neutron star formation as short γ-ray burst progenitors (Belczynski et al. 2006).

2.2   Dynamical events

2.2.1   Binary formation via physical collisions with giants

We consider in our models the possiblity of (eccentric) binary formation via physical collisions involving a red giant (RG). For binaries formed through NS–RG collisions, the final binary separation $a_{\rm f}$ and eccentricity $e_{\rm f}$ depend on the closest approach distance p (Lombardi et al. 2006) and can be estimated using the results of hydrodynamic calculations as

$$e_{\rm f} = 0.88 - \frac{p}{3R_{RG}} \qquad (2)$$

$$a_{\rm f} = \frac{p}{3.3(1 - e_{\rm f}^2)} \qquad (3)$$

More details on our treatment of these collisions can be found in Ivanova et al. (2006).

2.2.2   Collisions and mergers with NSs

We assume that the amount of matter accreted by a NS following a merger or collision depends on the evolutionary stage of the other star. If a NS collides or merges with a MS or a He MS star, we assume that it accretes no more that 0.2 $M_\odot$ (Rosswog 2006). In the case of a collision with a giant-like star, the maximum accreted mass is 0.01 $M_\odot$ (Lombardi et al. 2006). When the other star is a WD, all the WD mass is accreted. In essentially all mergers and collisions, the accreted mass must have gone through an accretion disk, implying that, if a significant amount of matter is accreted, a recycled pulsar will be formed.

2.2.3   Triples and their treatment

Stable hierarchical triples can be formed through binary–binary encounters. Although these triples would be stable in isolation, it is likely that they will be destroyed during their next dynamical encounter. As there are no developed population synthesis methods for handling triple star evolution, we cannot keep these triples in our simulations and instead we have to break them immediately after formation into a binary and a single star. We do this while conserving energy: the energy required to eject the outer companion is balanced by shrinking the inner binary orbit. The outer companion is released unless the required energy is such that the inner binary merges. In the latter case the inner system is allowed to merge and the outer companion is kept in a new, wider orbit to form the final binary system.

It is possible that in a triple the inner orbit's eccentricity will be increased via the Kozai mechanism (Kozai 1962). This secular coupling causes large variations in the eccentricity and inclination of the orbits and could drive the inner binary of the triple system to merge before the next dynamical interaction. The maximum eccentricity in systems with large initial inclinations i_0, such that $\sin i_0 > (2/5)^{1/2}$ ($i_0 \gtrsim 39°$) is (e.g., Innanen et al. 1997; Eggleton & Kiseleva-Eggleton 2001):

$$e_{\rm max} \simeq \sqrt{1 - 5/3\cos^2(i_0)} \,. \qquad (4)$$

The period of the cycle to achieve $e_{\rm max}$ is (Innanen et al. 1997; Miller & Hamilton 2002)

$$\tau_{\rm Koz} \simeq \frac{0.42\ln(1/e_{\rm i})}{\sqrt{\sin^2(i_0) - 0.4}} \left(\frac{m_1 + m_2}{m_{\rm o}}\frac{b_{\rm o}^3}{a_{\rm i}^3}\right)^{1/2} \left(\frac{b_{\rm o}^3}{Gm_{\rm o}}\right)^{1/2}, \qquad (5)$$

where $e_{\rm i}$ is the initial eccentricity of the inner binary, m_1, m_2 and m_o are the masses of the inner binary companions and the mass of the outer star, $a_{\rm i}$ and $a_{\rm o}$ are initial orbital separations for the inner and outer orbits, and $b_{\rm o} = a_{\rm o}(1 - e_{\rm o})^{3/2}$ is the semiminor axis of the outer orbit.

We compare the Kozai time-scale $\tau_{\rm Koz}$ with the collision time $\tau_{\rm coll}$ (computed as in Ivanova et al. 2005):

$$\tau_{\rm coll} = 8.5 \times 10^{12} \,\text{yr} \; P_{\rm td}^{-4/3} M_{\rm tot}^{-2/3} n_5^{-1} v_{10}^{-1} \times \qquad (6)$$

$$\left(1 + 913\frac{(M_{\rm tot} + \langle M \rangle)}{kP_{\rm td}^{2/3}M_{\rm tot}^{1/3}v_{10}^2}\right)^{-1}$$

Here $P_{\rm td}$ is the triple period in days, $M_{\rm tot}$ is the total triple mass in $M_\odot$, $\langle M \rangle$ is the mass of an average single star in $M_\odot$, $v_{10} = v_\infty/(10\,\text{km/s})$ and $n_5 = n/(10^5\,\text{pc}^{-3})$, where n is the stellar number density.

If $\tau_{\rm Koz} > \tau_{\rm coll}$, the Kozai mechanism does not affect the triple evolution before the next encounter occurs, and we break the triple as describe above. However, for triples with $\tau_{\rm Koz} < \tau_{\rm coll}$, we consider the circularization time-scale $\tau_{\rm circ}$ (see §3.3 in Belczynski et al. 2007). The characteristic time-scale for the inner binary separation to decrease through tidal dissipation is $\tau_{\rm circ}/2e_{\rm i}^2$ (Mazeh & Shaham 1979). If $\tau_{\rm circ}/2e_{\rm i}^2 < \tau_{\rm coll}$, the inner binary will shrink until one of the components overfills its Roche lobe or its separation will small enough to cause the Darwin instability resulting in a merger (Eggleton & Kiseleva-Eggleton 2001). In the opposite case, when $\tau_{\rm circ}/2e_{\rm i}^2 > \tau_{\rm coll}$, we assume that mass transfer starts if $e_{\rm max}$ is such that at least one of the stars in the inner binary overfills its Roche lobe at pericentre. As a result, triple formation may enhance the formation of mass-transferring binaries with a NS.

For sufficiently compact inner binaries, relativistic effects may play an important role. The relativistic precession period P_{pr} of the inner binary, to first post-Newtonian order, is (see Weinberg 1972, p.197):

$$P_{\mathrm{pr}} = \frac{2\pi c^2 a^{5/2}(1-e_{\mathrm{i}}^2)}{3G^{3/2}(m_1+m_2)^{3/2}} \qquad (7)$$

If $\tau_{\mathrm{Koz}} > P_{\mathrm{pr}}$, Kozai cycles are strongly suppressed (Holman et al. 1997).

We expect that some dynamically formed triples can also undergo significant secular eccentricity evolution even for orbital inclinations smaller than the Kozai angle (see e.g. Ford et al. 2000), but here we neglect this possibility.

2.3 Millisecond pulsars

In our standard model, MSPs are identified with NSs that have been spun up and had their magnetic fields reduced during an accretion phase (van den Heuvel 1984). The amount of material that needs to be accreted on to a NS to form a MSP is not established firmly. In our simulations we assume that in order to spin up to a millisecond period, a NS must accrete at least 0.01 $M_\odot$. We distinguish mass gain through steady accretion from that which can result from a physical collision (see also §2.2.2) or a CE event.

The time over which a MSP will spin down from its initial period P_0 to a current period P is

$$\tau_{\mathrm{MSP}} = \frac{P^2 - P_0^2}{2}\frac{1}{P\dot{P}}, \qquad (8)$$

where $P\dot{P} = B^2/10^{39}$ [s]. With the assumption that the magnetic field B does not decay, $P\dot{P}$ remains constant with time.

Several radio pulsars in GCs are slowly spinning ($P > 0.1$s) and have high $\dot{P}$s (higher than can be produced by gravitational acceleration in the cluster potential) implying relatively high B fields, $> 10^{11}$-gauss. These include NGC 6342A (van Kerkwijk et al. 2000), NGC 6624B (Biggs et al. 1994), and NGC 6440A Lyne et al. (1996). Their inferred characteristic ages range from 10^7 yr to 2×10^8 yr, compared to $10^{11} - 10^{13}$ yr for "normal" MSPs. The inferred birthrate for this class of objects is similar to that of "normal" MSPs, but observationally they seem to be concentrated in the densest clusters, and 2 of 3 are isolated pulsars. Several other pulsars in clusters may also be produced through a related mechanism; these include the numerous isolated MSPs in M15, and the isolated young pulsars NGC 6624A and M28A, both of which appear to be above the "spin-up line" for MSP production (Biggs et al. 1994).

Strong magnetic field of $> 10^{11}$-gauss can be a result of the collapse, assuming flux conservation, of a typical magnetic WD with $B \sim 10^6$-gauss. Observed magnetic WDs typically have higher masses than nonmagnetic WDs(Wickramasinghe & Ferrario 2005), indicating that they may dominate the population of WDs that undergo AIC. Stellar dynamo theory supports the link between strong magnetic fields and massive WDs (Thompson & Duncan 1993). It is also possible that a strong magnetic field may be generated during the merger of a WD pair, where one or more WD had a strong magnetic field, leading to the production of 10^{12}-gauss magnetic fields, or even magnetar B field strengths of $10^{14} \div 10^{15}$-gauss (King et al. 2001; Levan et al. 2006; Chapman et al. 2006). MSPs formed with such high magnetic fields will have relatively short lifetimes, and thus will make up only a small portion of the observed globular cluster MSP population.

3 MODELS

Our "standard" cluster model has an initial binary fraction of 100 per cent. The distribution of initial binary periods is constant in the logarithm between contact and 10^7 d and the eccentricities are distributed thermally. We emphasize that about 2/3 of these binaries are soft initially (the initial binary fraction for hard binaries is about 20 per cent if the 1-D velocity dispersion is 10 km/s) and most very tight binaries are destroyed through evolutionary mergers. Our initial binary fraction is therefore comparable to the initial binary fractions that are usually adopted in N-body simulations, 10-15 per cent in hard binaries (soft binaries are short-lived in dense clusters but slow down the calculations considerably). For a more detailed discussion of the choice of primordial binary fraction, see Ivanova et al. (2005).

For single stars and primaries we adopt the broken power law initial mass function (IMF) of Kroupa (2002) and we assume a flat mass-ratio distribution for secondaries. The initial core mass is 5 per cent of the total cluster mass and no initial mass segregation is assumed (an average object in the core is as massive as an average cluster star). At the age of 11 Gyr, which we adpot as a typical age of a Galactic GC, the mass of such a cluster in our simulations is $\sim 2.2 \times 10^5 \ M_\odot$ for a metallicity of a typical metal-rich cluster ($Z = 0.005$) and is comparable to the mass of typical GCs in our Galaxy. In the case of a metal-poor cluster (Z=0.0005), the mass is $\sim 2.5 \times 10^5 \ M_\odot$. To make a comparison between cluster models of different metallicities we will show all results scaled to a cluster mass $2 \times 10^5 \ M_\odot$. As the metal-rich case observationally is more important – most of bright LMXBs and MSPs detected so far are located there, we take for our standard model the value $Z = 0.005$.

For our standard model we fix the core density at $n_{\mathrm{c}} = 10^5 \ \mathrm{pc}^{-3}$. The link to an observed luminosity density can be found using the number density-to-mass density ratio, which is our simulations $\sim 2 \ M_\odot^{-1}$ at the ages of 7-14 Gyr, and mass-to-light ratio, which on average is $\sim 2.3 \ M_\odot/L_\odot$ and is 2 $M_\odot/L_\odot$ for 47 Tuc (Pryor & Meylan 1993). We adopt a half-mass relaxation time $t_{\mathrm{rh}} = 1$ Gyr (Harris 1996). The characteristic velocities are computed for a King model with dimensionless central potential $W_0 = 7$ and the total mass of the model, giving a one-dimensional velocity dispersion $\sigma_1 = 10$ km/s and a central escape velocity $v_{\mathrm{esc}} = 40$ km/s. If, after an interaction or SN explosion, an object in the core acquires a velocity higher than the *recoil velocity* $v_{\mathrm{rec}} = 30$ km/s, the object is moved from the core to the halo. The ejection velocity for objects in the halo is $v_{\mathrm{ej,h}} = 28$ km/s. This standard model represents a typical dense globular cluster in our Galaxy.

In addition to this "standard" model we also considered cluster models with the following modifications:

- a metal-poor cluster with $Z = 0.0005$ – "metal-poor";
- different central densities: $n_{\mathrm{c}} = 10^6 \ \mathrm{pc}^{-3}$, $n_{\mathrm{c}} = 10^4 \ \mathrm{pc}^{-3}$ and $n_{\mathrm{c}} = 10^3 \ \mathrm{pc}^{-3}$ – "high-dens", "med-dens" and "low-dens" respectively;
- a cluster with smaller velocity dispersion and smaller ejection velocity – "low-σ";
- shorter half-mass relaxation time "long-t_{rh}";
- reduced initial binary fraction, $f_{\mathrm{b}}^0 = 50$ per cent – "BF05";
- magnetic braking taken as in Rappaport et al. (1983) – "fast MB";
- reduced efficiency of the common envelope, $\alpha_{\mathrm{CE}}\lambda = 0.1$ – "CE-reduced";
- natal kick distribution is doubled peaked Maxwellian as in Arzoumanian et al. (2002) – "oldkicks"

Table 1. Models.

	$n_{\rm c}$	$t_{\rm rh}$	Z	σ_1	$v_{\rm esc}$	$f_{\rm b}^0$	$\alpha_{\rm CE}\lambda$	MB	$M_{\rm cluster}$	Runs (number of stars)
standard	10^5	1.0	0.005	10	40	100%	1.0	IT03	$2 \times 10^5 M_\odot$	5 with 10^6, 5 with 2×10^6
metal-poor	·	·	0.0005	·	·	·	·	·	·	5 with 10^6
high-dens	10^6	·	·	·	·	·	·	·	·	5 with 10^6
med-dens	10^4	·	·	·	·	·	·	·	·	5 with 10^6
low-dens	10^3	·	·	·	·	·	·	·	·	5 with 10^6
low-σ	·	·	·	5	20	·	·	·	·	5 with 10^6
long-$t_{\rm rh}$	·	3.0	·	·	·	·	·	·	·	5 with 10^6
BF05	·	·	·	·	·	50%	·	·	·	5 with 10^6
fast-MB	·	·	·	·	·	·	·	RVJ	·	5 with 10^6
CE-reduced	·	·	·	·	·	·	0.1	·	·	5 with 10^6
oldkicks	·	·	·	·	·	·	·	·	·	5 with 10^6
47 Tuc	$2.5 \cdot 10^5$	3.0	0.0035	11.5	57	·	·	·	$10^6 M_\odot$	5 with 2×10^6
Terzan 5	$8 \cdot 10^5$	0.93	0.013	11.6	49	·	·	·	$3.7 \times 10^5 M_\odot$	5 with 1.7×10^6

Notations: $n_{\rm c}$ – core number density (pc^{-3}); $t_{\rm rh}$ – half-mass relaxation time (Gyr); Z – metallicity; σ_1 – one-dimensional velocity dispersion (km/s); $v_{\rm esc}$ – central escape velocity (km/s); $f_{\rm b}^0$ – initial binary fraction (see text for corresponding binary fraction of hard binaries); $\alpha_{\rm CE}\lambda$ – CE efficiency; MB – adopted prescription for magnetic braking (IT03 is from Ivanova & Taam (2003) and RVJ is from Rappaport et al. (1983)); $M_{\rm cluster}$ – all the results for this model are scaled to this adopted cluster mass. "Oldkicks" model uses the distribution of natal kick velocities from (Arzoumanian et al. 2002). Symbol "·" means that the value is the same as in the standard model.

• 47 Tuc-type cluster, characterized by a higher density $n_{\rm c} = 10^{5.4}\,{\rm pc}^{-3}$ (with M/L=2 as in (Pryor & Meylan 1993) it corresponds to $\rho_{\rm c} = 10^{4.8}\,L_\odot\,{\rm pc}^{-3}$ as in Harris (1996)) , metallicity $Z = 0.0035$, $t_{\rm rh} = 3$ Gyr (Harris 1996) $\sigma_1 = 11.5$ km/s (Pryor & Meylan 1993), $v_{\rm esc} = 57$ (Webbink 1985), with the recoil velocity of 51 km/s and $v_{\rm ej,h} = 32$ km/s (King model $W_0 = 12$)) – "47 Tuc";

• Terzan 5 cluster, $n_{\rm c} = 10^{5.9}\,{\rm pc}^{-3}$ ($\rho_{\rm c} = 10^{5.23}\,L_\odot\,{\rm pc}^{-3}$ as in Heinke et al. (2003)), metallicity $Z = 0.013$ (Origlia & Rich 2004), $t_{\rm rh} = 0.9$ Gyr (Harris 1996) $\sigma_1 = 11.6$ km/s, $v_{\rm esc} = 49.4$ (Webbink 1985), with the recoil velocity of 39 km/s and $v_{\rm ej,h} = 29$ km/s (King model $W_0 = 8.3$) – "Terzan 5".[3]
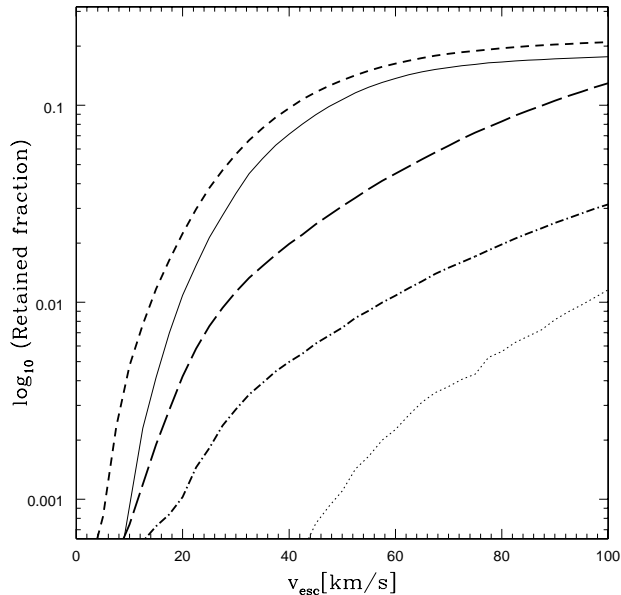
For the complete list of models see Table 1.

We expect that only a few LMXBs can be formed in every cluster with a typical mass of 200,000 $M_\odot$ through 11 Gyr of dynamical evolution, and therefore we perform 5 runs for each model with 10^6 initial stars and for the standard models - five runs with 2×10^6 stars, to check that statistics for rare objects like LMXBs is not different when the resolution is increased (for most of our results presented below we did not find statistical differences between high and low resolution models, and fluctuations for the rate events are smaller in the case of high resolution). For Terzan 5 and 47 Tuc models, though, we do all runs at high resolutions. In particular, in the case of Terzan 5 1.7×10^6 stars provide at 11 Gyr the mass comparable to the estimated observed mass of 370,000 $M_\odot$. In the case of 47 Tuc the reason for a higher resolution is that the relative core mass is smaller than in the case of a standard cluster, due to longer $t_{\rm rh}$.

Table 2. Production of NSs, field population.

	CC	ECS	AIC	MIC	$N_{40}^{\rm cc}$	$N_{40}^{\rm tot}$	$N_{\rm NS}$
single							
Z=0.0005	3354	594	-	-	2.1	251	584848
Z=0.001	3255	581	-	-	1.9	245	565168
Z=0.005	2833	570	-	-	1.2	243	498513
Z=0.02	2666	400	-	-	1.2	172	424696
oldkicks	2730	-	-	-	19.3	19.3	339669
binary							
Z=0.0005	3079	545	59	14	19	329	249775
Z=0.001	3056	553	60	15	15	332	242601
Z=0.005	2750	576	58	16	14	335	219236
Z=0.02	2463	406	33	20	12	240	180582
oldkicks	2929	-	-	-	58	58	237705

Notations for channels – CC - core-collapse supernova; ECS - electron-capture supernova; AIC - accretion induced collapse; MIC - merger-induced collapse. Numbers are scaled per 200,000 $M_\odot$ stellar population mass at the age of 11 Gyr. $N_{40}^{\rm cc}$ and $N_{40}^{\rm tot}$ are the retained numbers of NSs formed via core-collapse and through all channels, if the escape velocity is 40 km/s. $N_{\rm NS}$ are the total numbers of formed NSs in simulated populations.

4 NEUTRON STAR FORMATION AND RETENTION

4.1 Formation

To estimate how many NSs can be formed and retained in GCs, we first studied stellar populations without dynamics, considering separately populations with only primordial single stars and only primordial binaries. We considered several metallicities – from solar (as in the Galactic field) to that of a typical metal-poor cluster: Z=0.02, 0.005, 0.001, 0.0005. In addition, we also studied for comparison a model (with Z=0.005) with the previously accepted natal kick distribution, 2 Maxwellians with a lower peak for kick ve-

---

[3] The recent study of Ortolani et al. (2007) suggests a shorter distance, and thus higher central density for Terzan 5 ($\rho_{\rm c} = 10^{5.61} L_\odot/{\rm pc}^3$). If this study is correct, then Terzan 5's characteristics may be more closely approximated by our "high-density" cluster.

Figure 1. The retention fractions as a function of escape velocity (for stellar evolution unaffected by dynamics). Dotted and dash-dotted lines show the retention fractions for single and binary populations, core-collapse NSs only. Solid and short-dashed lines show the total retention fractions for single and binary populations, all NSs. Long-dashed line shows the total retention fraction of a binary population with the old kick distribution.

locities at 90 km/s (Arzoumanian et al. 2002). The results for NS production via different channels are shown in Table 2.

The production of NSs via core-collapse SNe (CC NSs), per unit of total stellar mass at 11 Gyr, decreases as metallicity increases. The difference between the Galactic field case and a metal-poor case is about 20 per cent, while the difference between metal-rich and metal-poor clusters (Z=0.005 and Z=0.0005) is about 10-15 per cent, for primordial single or binary populations.

ECSe in single stars for metal-rich populations occurs in stars of higher masses. The range of initial masses is, however, the same for both populations and is about $0.6M_{\odot}$. As a result, the number of NSs produced via ECSe (ECS NSs) from the population of single stars is smaller in the case of a Galactic field population than in the case of a GC population by 30 per cent, while the difference between metal-rich and metal-poor clusters is only 5 per cent. This is in complete agreement with the adopted power law for the IMF. In binaries, the mass interval where ECSe could occur is expanded compared to single stars of the same metallicity. This difference is large enough that metal-rich clusters produce more ECSe than metal-poor clusters.

NSs produced via AIC and MIC also have similar production rates in metal-rich and metal-poor populations. We note that MICs give the smallest contribution to the production of NSs in populations evolved without dynamics.

4.2 Retention

In Fig. 1 we show the retention fraction of NSs at formation as a function of the central escape velocity, considering populations of metal-poor primordial singles and binaries; CC NSs and the whole NS population are shown separately. It can be seen that, with the adopted natal kick distribution, CC NSs from a single star pop-

ulation are rarely retained (see also Table 2). In a population of primordial binaries, the fraction of retained CC NSs is higher than for single stars. None the less, the resulting number of retained CC NSs is significantly smaller than we get from the other NS formation channels. We conclude that if indeed ECS, AIC or MIC are not accompanied by a large natal kick, the total number of retained NSs is high and only a negligible number of CC NSs is present. As the ECS NS masses are only $1.26M_{\odot}$, this may lead to a NS mass function skewed towards low values.

With the old distribution for natal kick velocities, reasonable numbers of NSs can be produced and retained in a typical GC, while a massive cluster like 47 Tuc could retain as many as 600 NSs (see also Fig. 1). This result agrees with the retention fractions obtained in Pfahl et al. (2002).

4.3 Effects of dynamics

The effects of dynamics on the production and retention of NSs are illustrated in Table 3. The number of formed CC and ECSs NSs is in agreement with the retained fraction of the stellar population where binaries have been partially depleted and some of the SN progenitors were located in the halo, where the escape speed is lower than in the core. We find that the production of NSs via AIC and MIC is strongly enhanced by dynamical encounters compared to a field population. As a result, those formation channels together become comparable to the ECS channel, and produce many more retained NSs than the CC channel. A metal-poor cluster, following the trend of field populations, possesses a few per cent more NSs.

As noted before, MIC could lead to the formation of magnetars, which also appear as anomalous X-ray pulsars (AXPs). Currently, there are no AXPs detected in old GCs, and only one AXP is detected in a young "super star cluster," Westerlund 1 (Israel et al. 2007). On the other hand, all known AXPs are younger than 10^5 yr. In this case, AXPs could be found in GCs only if their formation rate is above 1 per 200 (GCs) per 10^5 yr, or at least 500 per typical cluster, over the cluster lifetime. Our formation rates are significantly smaller and therefore the hypothesis of a MIC connection to AXPs does not contradict our results.

4.4 Location

We consider the position of retained NSs in the cluster. The progenitors of CC NSs are mainly massive stars with masses $\gtrsim 20M_{\odot}$. However a significant fraction of progenitors of ECSe, especially those that evolved from a primordial binary, have intermediate initial masses—as low as 4 $M_{\odot}$. The evolutionary time-scales for NSs to be formed are $\sim 10^7$ yr for an CC NS and $\sim 10^8$ yr for an ECS NS. These are only $\sim$ 2 per cent and $\sim$ 10 per cent, correspondingly, of the cluster half-mass relaxation time $t_{\rm rh}$, where $t_{\rm rh} = 10^9$ yr in a typical cluster. Even massive stars do not experience strong mass segregation during $\sim 0.02t_{\rm rh}$, the same is true for stars of intermediate masses that produce ECS NSs (see, e.g., Fig.7 in Gürkan et al. 2004, , where the mass segregation with time in a cluster with stars between 0.2 $M_{\odot}$ and 120 $M_{\odot}$ is shown). When a NS is formed, the mass of the star is significantly decreased. As a result, a significant fraction of NSs is formed in the halo, and many will remain there. As many as $\sim$ 60 per cent of all ECS NSs in the case of a typical cluster ($t_{\rm rh} = 10^9$ yr) remain in the halo at 11 Gyr. AIC and MIC NSs are also present in the halo, but in a lesser proportion, as they are mainly produced in a dense environment. Many of the halo AIC and MIC NSs have recoiled from the core as

Table 3. Retained NSs and their locations at 11 Gyr, for different globular cluster models.

model	Core				Halo			
	CC	ECS	AIC	MIC+CIC	CC	ECS	AIC	MIC+CIC
standard	3.5 ± 1.5	65.6 ± 9.3	21.1 ± 3.7	10.3 ± 4.0	4.8 ± 1.7	91.4 ± 11	18.0 ± 3.9	9.7 ± 1.7
metal-poor	3.6 ± 1.7	71.5 ± 12	30.4 ± 3.2	8.4 ± 4.5	2.3 ± 1.1	91.7 ± 9.2	20.9 ± 4.8	10.9 ± 3.8
high-den	3.3 ± 1.7	65.5 ± 7.8	42.7 ± 5.8	20.7 ± 6.1	4.2 ± 3.3	111 ± 12	29.0 ± 5.2	12.8 ± 3.4
med-den	3.3 ± 2.1	63.7 ± 5.2	18.6 ± 4.5	6.4 ± 3.0	4.8 ± 1.5	85.6 ± 8.0	14.3 ± 3.1	9.4 ± 3.7
low-den	3.2 ± 1.3	65.1 ± 5.9	14.2 ± 3.3	9.8 ± 0.9	3.8 ± 1.3	91.2 ± 11	15.4 ± 2.1	7.0 ± 2.0
low-σ	0.5 ± 0.8	15.5 ± 3.2	5.5 ± 2.3	10.7 ± 2.5	0.9 ± 1.1	19.4 ± 4.2	4.3 ± 1.7	11.5 ± 1.8
long-$t_{\rm rh}$	1.4 ± 1.0	30.0 ± 4.7	9.3 ± 2.1	3.0 ± 1.2	5.3 ± 0.9	124 ± 15	22.5 ± 5.5	15.5 ± 3.3
BF05	1.8 ± 1.2	64.1 ± 5.0	15.0 ± 3.1	6.7 ± 2.5	3.9 ± 1.0	88.6 ± 6.7	11.4 ± 2.7	6.2 ± 1.7
fast-MB	3.8 ± 1.6	77.3 ± 6.0	22.9 ± 3.3	10.6 ± 4.3	5.1 ± 1.9	93.7 ± 6.9	17.2 ± 3.3	8.3 ± 3.2
CE-reduced	2.9 ± 1.9	72.2 ± 5.6	12.7 ± 2.8	9.4 ± 1.9	3.6 ± 2.6	99.2 ± 4.0	4.5 ± 1.7	11.7 ± 1.9
oldkicks	14.6 ± 3.9	0.0 ± 0.0	0.0 ± 0.0	0.3 ± 0.4	21.3 ± 4.0	0.0 ± 0.0	0.0 ± 0.0	0.0 ± 0.0
47 Tuc	11.8 ± 7.5	215 ± 20	91.8 ± 23	27.7 ± 8.0	38.3 ± 7.9	598 ± 41	102 ± 4.9	69.3 ± 12
Terzan 5	5.1 ± 1.4	132 ± 8.9	91.9 ± 11	47.8 ± 4.6	8.9 ± 1.4	143 ± 10	38.0 ± 6.6	22.7 ± 4.5

Notations for channels as in Table 2. For all GC models, except 47 Tuc and Terzan 5, the numbers are scaled per 200 000 $M_\odot$ stellar population mass at the age of 11 Gyr; for 47 Tuc the numbers are given per its total mass taken as 10^6 $M_\odot$, for Terzan 5 - per 370 000 $M_\odot$. Numbers show the results averaged over all runs for each cluster model (for the number of runs see Table 1).

a result of dynamical encounters. A significant difference with the distribution of NSs over the clusters can only be expected for initial mass segregation, or if the initial $t_{\rm rh}$ was much shorter than the current $t_{\rm rh}$ resulting in faster mass segregation at early stages. Observations find (e.g. Grindlay et al. 2002) that the radial distribution of MSPs within globular clusters in 47 Tuc is consistent with the production of all MSPs within the core (but cf. Gürkan & Rasio 2003).

5 FORMATION OF BINARIES WITH NEUTRON STARS

5.1 Primordial binaries with NSs

The probability for a NS to remain in a primordial binary depends strongly on its formation channel (see Table 4). By definition, MIC leads to the formation of a single NS star. AIC occurs in a very tight binary. Accordingly, a NS formed this way will most likely remain in a binary. Among CC NSs or ECS NSs, only several per cent remains in binaries immediately after NS formation. A survived post-SN binary has a relatively massive secondary that is also likely to experience SN or the binary may evolve through dynamically unstable mass transfer resulting in the merger, with stringer binary depletion in the case of more massive initially binaries with a CC NS. As a result, very little of NS binaries formed through those channels eventually remain in binaries. Most likely for a primordial binary in a GC to contain a NS is in the case of a post-AIC binary. Low probability for CC NSs and ECS NSs to be members of a primordial binary does not change strongly with the change of the metallicity.

The formation rate of AIC NSs in GCs shows that as many as 40 NS-MS binaries can be formed in a typical cluster. Most of them will evolve through LMXB stage before the age of 11 Gyr, producing in the result 20-30 recycled pulsars, although those MSPs could be very short living and be not observed today (see §2.3). Overall, NSs that remain in binaries may evolve through the mass-transfer phase, but most of such events occurs very early in the evolution, mainly within first 2 Gyr. In more details, per sample of 270 000 NSs formed from primordial binaries (Z=0.005), none of binaries started the MT with a MS star after the stellar population reached

Table 4. Binary fractions for NSs in primordial binaries.

Z	after NS formation			at 11 Gyr		
	CC	ECS	AIC	CC	ECS	AIC
0.0005	2.9%	3.0%	92.3%	0.28%	1.38%	78.6%
0.001	2.8%	3.4%	93.6%	0.25%	1.41%	81.8%
0.005	2.6%	3.4%	96.0%	0.18%	1.54%	88.0%
0.02	1.4%	4.2%	95.2%	0.12%	1.49%	85.9%

The fractions of NSs that remain in primordial binaries immidiately after NS formation (columns 2 ÷ 4) and at 11 Gyr (columns 5 ÷ 7), for each formation channel.

the age of 8 Gyr; for the ages between 10 and 11 Gyr we encountered only 1 LMXB with a RG and 2 LMXBs with a WD. From this stellar population runs it is clear that it is highly unlikely that LMXBs observed in GCs of our Galaxy today are primordial. An exception to this can occur only if a primordial binary had participated in an encounter, retained its both companions, but changed binary separation and/or eccentricity, resulting in the mass transfer at older cluster ages.
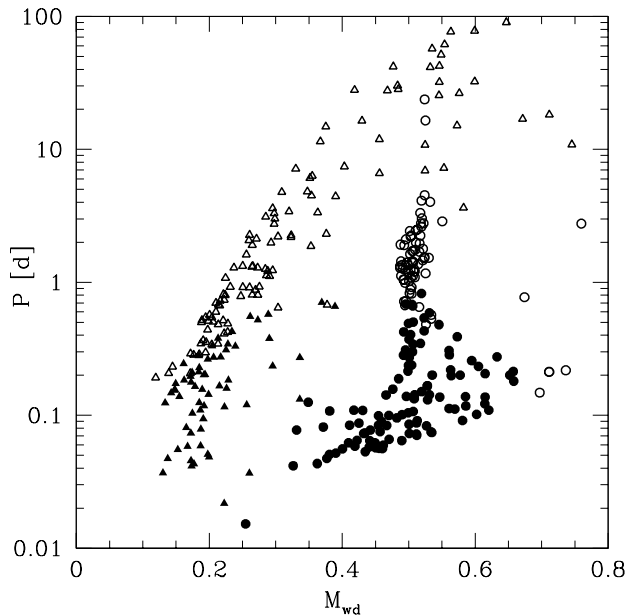
The number of double neutron star (DNS) systems formed in a field is very low, typically just a few DNSs per 200,000 $M_\odot$ at 11 Gyr. For a typical GC this number will be smaller since some of the primordial binaries will be destroyed dynamically and most DNSs will be ejected. In fact, more than 99 per cent of NSs that were formed first are CC NSs, and, accordingly, had a high natal kick. Formation of primordial DNSs occurred very early in the GC evolution. Most of them are very tight and merge quickly, leaving very little chance for one to be observed today. As this paper only uses the results of the NS formation and evolution in the field as a reference point, we refer the reader to the complete study of DNS formation channels from primordial binaries, rates, appearance with time, metallicity dependence and other details provided in (Belczynski & et al. 2007). We conclude that essentially no primordial DNS can be present in a Galactic GC at the current time.

Table 5. NS binaries formed in scattering experiments.

	Z	σ	PC		TC	
		km/s	Tot	MT	Tot	MT
standard	0.005	10	3.68%	1.75%	2.35%	1.20%
metal-poor	0.0005	10	3.25%	1.30%	1.93%	0.95%
low-σ	0.05	5	6.80%	3.61%	9.24%	4.37%

The table shows the fraction of NSs that successfully formed a binary via physical collision (PS) or tidal capture (TC). Tot is the total number and MT is the fraction of NSs that not only formed a binary, but also started mass transfer before 11 Gyr.

Figure 2. Companions in binary systems formed via physical collision with a red giant during the scattering experiment (Z=0.001). Triangles are WDs, circles are He stars; solid symbols denote the systems that started the mass tranfer before 11 Gyr.

5.2 Physical collisions

A binary with a NS and a WD can be formed via physical collision with a giant (see §2.2.1). This binary formation mainly works during single-single star collisions, although it may occur during a binary-single encounter as well. As we shown above, the number of NSs that can be retained in globular clusters is about couple of hundreds per a typical globular cluster. Let us estimate the rate of the encounter. The cross-section for two stars that have a relative velocity at infinity v_∞ to pass within a distance r_{max} is

$$\sigma = \pi r_{min}^2 (1 + \frac{2G(m_1 + m_2)}{r_{max} v_\infty^2}) , \qquad (9)$$

where the second term is gravitational focussing and in, stellar systems with low velocity disperion loke GCs, it exceeds the first term. The time-scale for a NS to undego an encounter with a red gaint can be estimated as $\tau_{coll} = 1/f_{RG} n \sigma v_\infty$, where f_{RG} is the relative fraction of red giant in the stellar population:

$$\tau_{coll} = 1.6 \times 10^{11} \text{ yr } v_{10} n_5^{-1} (M_{NS} + M_{RG})^{-1} R_{max}^{-1} f_{RG}^{-1} , \quad (10)$$

where M_{NS} and M_{RG} are masses of a NS and a red giant in $M_\odot$ and $R_{max} = r_{max}/R_\odot$ is the maximum distance between the stars during the encounter that leads to the binary formation. Lombardi et al. (2006) shown that $r_{max} \approx 1.5 R_{RG}$, where R_{RG} is the radius of the red gaint. An averaged with time R_{RG} is about few solar radii (Ivanova et al. 2005), and $f_{RG} \approx 5$ per cent. Using eq. (10) we estimate that during 11 Gyr about 5 per cent of NSs can participate in binaries formation through physical collisions.

As the estimate shows, having about 200 NSs in our models of GCs (and about 400 for models with the largest resolution, 2×10^6 stars), we can form maximum 10 binary systems through the whole cluster simulation. To study statistically the characteristics of post-encounter binaries, we made the scattering experiment as the following: we considered the population of 10^6 single stars, with an IMF from $0.2 M_\odot$ to $3.0 M_\odot$ and 10000 NSs of $1.4 N_\odot$. All stars are initially placed in the core with $n_c = 10^5$ pc^{-3}. We considered three different models - with the standard and low metallicities, and with low velocity dispersion (see also Table 5). In these simulations only single-single encounters were allowed.

The scattering experiment shows that 3.7 per cent of all NSs participated in a successful binary formation via physical collision with a RG or an AGB star. This fraction slightly decreases when the metal-poor population is considered and increases by a factor of about 2 (in accordance with eq. 10) in the case of the lower velocity dispersion. The fraction of NS–WD systems that started MT before 11 Gyr is high, ~ 50 per cent (see Table 5).

Let us consider what are the companions of NSs in these binaries. On Fig. 2 we show masses of companions in post-collision binaries versus orbital periods. We form about the same number of systems with WD companions and stripped He stars companions (from collisions with AGB stars). Systems with He star companions are mainly formed within first 2 Gyr and start the MT mostly within 3 Gyr. After about 3 Gyr both the formation rate and and the appearance rate is slightly higher for systems with WD companions The evolution of mass-transferring systems with a He star companion is a bit different from those with a WD companion. They are a few times wider (for the same companion mass) and do not live as long in the mass-transferring phase at high luminosities.

In our numerical simulation of different models of GCs the actual rates are smaller. For instance, not all NSs are immediately present in the core at the time of their formation, and about half of them are still in the halo at the age of 11 Gyr. As a result, our "standard" model shows about 2 per cent formation rate per NS present in the core (or 1 per cent per all NSs in the cluster), producing only 2 systems. The scatter between several realizations is big. In some simulations we had formed twice less binaries via this channel, and, in one simulation, 3 times more of the average binary systems was formed. For a standard model, none of simulations had no binary formed. We note that low-σ cluster model, unlike the scattering results, does not produce twice more NS-WD binaries than a standard – low-σ cluster retains less of NSs that standard.

5.3 Tidal captures

In our previous study, devoted to the formation of cataclysmic variables (CVs) in globular clusters (Ivanova et al. 2006), we found that the tidal captures play a relatively small role in the whole dynamical binaries formation, only $\sim 1 - 2$ per cent of the total formation rate. Two main reasons were responsible for this: (a) a significant fraction of CVs have been formed directly from primordial binaries and (b) both physical collisions and exchange encounters occurred with a less massive than a NS objects form tighter binaries, increas-

ing their chance to start the MT. For the case of tidal captures with NSs, the results are different.

At first, we analyze the results of the scattering experiments which are set up as described before. We find that only ∼ 2 per cent of NSs have formed a binary via TC (see Table 5); with small decrease in the case of metal-poor population and with 4 times increase in the case of the lower velocity dispersion. The latter is explained as in the case of the tidal captures $r_{\max}$ is also the function of the velocity and is increasing as the relative velocity decreases (for more details, see Ivanova et al. (2006)).

The rate of tidal captures is flat both with time and the companion mass. In the case of metal-poor population, almost only TC systems formed before 5 Gyr have started the MT before the cluster age of 11 Gyr. In the case of our standard metal-rich population, only some systems with MS companions $> 0.85 M_\odot$ started the MT before 11 Gyr being formed with few last Gyr. We conclude that < 1 per cent of NSs can form a LMXB via tidal captures and the number of LMXB mainly depends not on the current cluster properties, but on the dynamical conditions in the cluster core more that 5 Gyr ago. In the case of metal-rich clusters, there is exception for initially more massive MS companions.

In our numerical simulations the formation rate is even smaller, due to the same reasons as in §5.2. An average probability in our "standard" model for a NS to participate in a TC is 0.6 per cent and two times less to form an LMXBs via this channel. None the less, even being very small, TC formation channel for LMXBs is comparable to that of physical collisions (see for more details §6).

5.4 Exchange encounters

As can be seen from eq. 10, due to a larger $r_{\max}$, binary encounters are much more likely than single star collisions. However, compared to the case of physical collisions and TC, where very tight binaries are formed, a smaller fraction of the successful exchange encounters is expected to result in the MT binary. The reason is that when the binary exchange occurs, the binary separation in the formed post-exchange binary roughly scales with the pre-exchange binary separation as the ratio of the new companion mass to the mass of the replaced companion (Heggie et al. 1996). Therefore, when a single NS become a member of a binary system at the ages of several Gyrs, the post-exchange system expands, as the mass of the replaced companion is always less than a mass of a NS. In addition, when a binary encounter occurs with very tight binaries, those that would be likely to start the MT soon even in the case of post-exchange expansion, will more likely collide during the binary encounter instead of result in the exchange (Fregeau et al. 2004).

On overall, in our standard model ∼ 20 − 25 per cent of NSs in a cluster (40-50 per cent if consider only NSs in the core) will sucesfully form a binary through an exchange encounter, ∼ 80 per cemt of post-exchange binaries will have a MS companion, and ∼ 15 per cent – a WD companion. Only 1.5 per cent of NSs will form a MT binary with a MS companion, and only 0.2 per cent – with a WD companion. The role of binary exchanges in the formation of NS-WD LMXBs is therefore negligible compared to physical collisions.

6 LOW-MASS X-RAY BINARIES

From the discussion above, one can see that the expected formation rate of LMXBs is rather small. For all dynamical formation chan-

Table 7. Presence probability of LMXBs with different donors

model	MS	RG	WD
standard	1.847 ± 0.562	0.120 ± 0.158	0.684 ± 0.594
metal-poor	1.216 ± 1.053	0.096 ± 0.065	0.507 ± 0.643
high-den	7.312 ± 2.206	0.196 ± 0.270	8.222 ± 2.975
med-den	0.455 ± 0.404	0.026 ± 0.042	0.206 ± 0.381
low-den	0.507 ± 0.630	0.005 ± 0.011	0.113 ± 0.254
low-σ	3.134 ± 1.251	0.066 ± 0.062	0.493 ± 0.452
long-$t_{\rm rh}$	0.835 ± 0.735	0.089 ± 0.181	0.358 ± 0.494
BF05	1.116 ± 0.316	0.075 ± 0.116	0.747 ± 0.279
fast-MB	1.377 ± 0.931	0.102 ± 0.113	1.687 ± 1.061
CE-reduced	1.976 ± 1.332	0.064 ± 0.062	0.775 ± 0.555
oldkicks	0.287 ± 0.485	0.0	0.0
47 Tuc	9.280 ± 4.095	0.133 ± 0.088	7.718 ± 2.348
Terzan 5	7.160 ± 1.949	0.143 ± 0.115	13.582 ± 6.573

The table shows the probability of LMXB presence at ages 11 ± 1.5 Gyr, for different donors (RG includes also subgiants and Hertzsprung Gap stars).
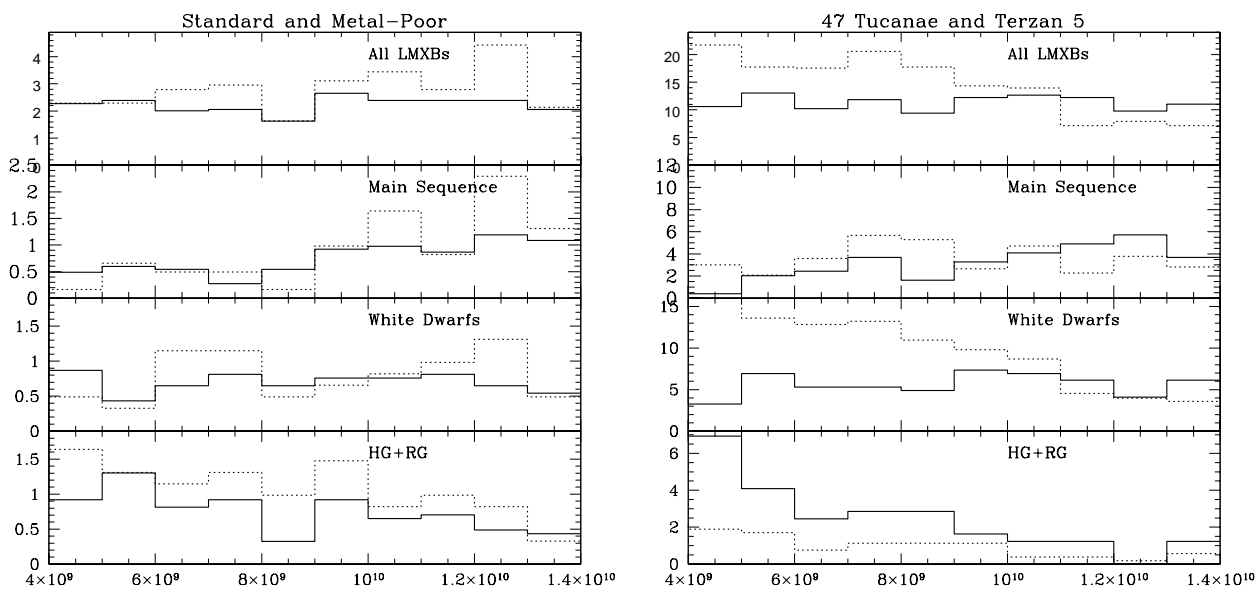
nels that involve a NS directly, in a typical dense metal-rich cluster, the combined rate is only ∼ 3 per cent per NS. This is 6 LMXBs per 11 Gyr of the cluster life, where 2 LMXBs are with a WD companion and 4 LMXBs are with a MS or a RG companion. There is a small number of LMXBs that may come from primordial, but dynamically modified binaries (where the encounters changed the binary eccentricity or separation). In addition, however, some fraction of LMXBs is expected to be provided by dynamically formed binaries with heavy WDs. Such binaries, if evolve through AIC, create a binary that reinstates MT on a NS soon after AIC occurred. The resulting post-AIC binary can have the MT with either MS, WD or RG donor. For all the details on the dynamical formation of WD-binaries, see Ivanova et al. (2006). From our current simulations, we find that the channel of LMXB production from AIC of dynamically formed WD binaries produces more LMXBs than all the dynamical LMXB production channels discussed above. On overall, in a typical cluster it is 2-3 times more efficient during 9.5-12.5 Gyr than physical collisions, tidal captures and binary exchanges (see Table 6). The exception only are very high density clusters. We note also that if this is indeed true, and if NSs formed through an AIC posses high magnetic field , then the production rate of LMXBs should not be expected to be coupled directly coupled with the number of observed MSPs, as the life-times of such MSPs is very short (see §2.3).

On Fig. 3 we show when LMXBs (with different companions) appear during the cluster evolution. We show only the cluster ages after 4 Gyr as before that mainly primordial LMXBs appear. The connection between the number of LMXBs that appeared at a certain time and those that are present at the same time in a GC is provided by the life-time $\tau_{\rm LMXB}$ of an LMXBs with the certain donor. An average $\tau_{\rm LMXB}$ for NS-MS LMXBs is about 1 Gyr. Depending on the metallicity and the initial donor mass, a system can be persistent 5-40 per cent of the MT time for metal-rich donors $> 0.6 M_\odot$ and transient at the rest; for donors of lower metallicities or smaller masses, a NS-MS LMXB will be transient at all the time (Ivanova 2006), and therefore most likely be seen as a qLMXBs rather than a bright LMXB. In the case of NS-WD LMXBs – an ultra-compact X-ray binary (UCXBs), total $\tau_{\rm LMXB}$ is few Gyr, however the time when a system is persistent and has X-ray luminosity above 10^{36} erg/s is 10^8 yr only. An LMXBs with a red giant companion or a companion that is in a Hertzsprung gap

Table 6. Average appearance rate of LMXBs formed via different dynamical channels.

model	AIC	TC	PC	BE/MS	BE/WD
standard	1.495 ± 0.537	0.070 ± 0.099	0.139 ± 0.172	0.512 ± 0.577	0.056 ± 0.098
metal-poor	2.402 ± 0.543	0.112 ± 0.153	0.056 ± 0.125	0.672 ± 0.730	0.0
high-den	3.624 ± 1.418	0.966 ± 0.755	1.266 ± 0.655	1.812 ± 0.706	0.0
med-den	0.540 ± 0.191	0.108 ± 0.148	0.0	0.108 ± 0.148	0.0
low-den	0.216 ± 0.226	0.0	0.0	0.0	0.0
low-σ	0.768 ± 0.444	0.060 ± 0.134	0.0	0.474 ± 0.265	0.058 ± 0.130
long-$t_{\rm rh}$	0.866 ± 0.676	0.0	0.0	0.108 ± 0.148	0.054 ± 0.121
BF05	1.204 ± 0.518	0.050 ± 0.112	0.100 ± 0.224	0.400 ± 0.137	0.0
fast-MB	1.886 ± 0.362	0.056 ± 0.125	0.168 ± 0.153	0.888 ± 0.363	0.0
CE-reduced	1.322 ± 0.531	0.0	0.0	0.498 ± 0.229	0.0
oldkicks	0.0	0.0	0.0	0.112 ± 0.153	0.0
47 Tuc	8.030 ± 1.160	0.280 ± 0.626	0.560 ± 0.586	2.490 ± 0.356	0.140 ± 0.313
Terzan 5	9.350 ± 1.198	1.428 ± 0.493	2.205 ± 0.419	2.209 ± 0.701	0.129 ± 0.290

The table shows the number of LMXBs that appear per Gyr at ages 11 ± 1.5 Gyr, for different formation channels: AIC in a dynamically formed WD-binary, TC –tidal capture, PC– physical collision, BE/MS – binary exchanges when a MS companion is acquired, BE/WD – binary exchanges when a WD companion is acquired.

Figure 3. Number of appearing LMXBs per Gyr with different donor types (with all donors, with MS donor, with WD donors and with donors that are RG or subgiants or are in the Hertzsprung Gap). The left panel shows the results for standard model (solid line) and metal-poor model (dotted line). The right panel shows the results for 47 Tuc (solid line) and Terzan 5 (dotted line).
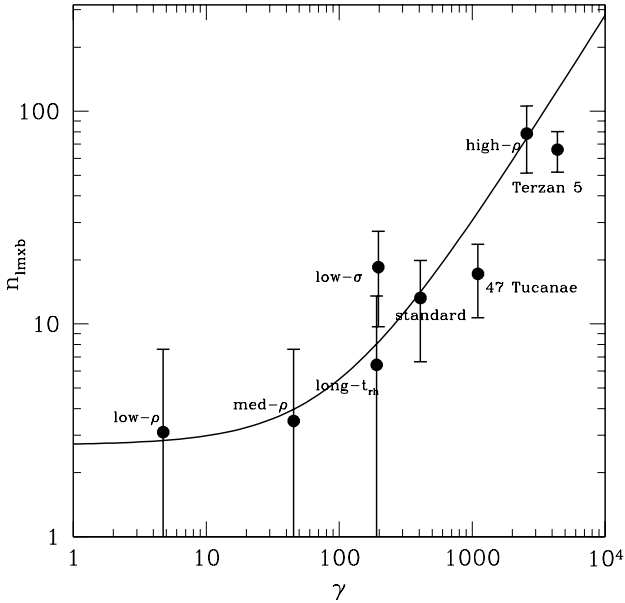
is very short-living, $10^5 - 10^7$ yr, and in only very rare cases they can leave as long as 10^8 yr.

Combining the number of appearing LMXBs with their life-times in the simulations, we find that a typical dense cluster at 11 ± 1.5 Gyr age can contain up to 2 LMXBs with a MS companion and up to 1 LMXB with a WD companion (see also Table 7, note very large scatter). As expected, the number of LMXBs shows a strong dependence on the core density; the dependence on the velocity dispersion and the half-mass relaxation time is also observed. We specify, that Table 7 shows the *presence* probability of LMXB – this is the probability to contain both bright LMXBs and qLMXBs.

A strong dependence of LMXB production on cluster density has been inferred observationally, both in Galactic globular clusters (e.g., Verbunt & Hut 1987; Pooley et al. 2003; Heinke et al. 2003)

and in extragalactic globular clusters (e.g., Jordán et al. 2004; Sivakoff et al. 2006). The interpretation has been that $N_{\rm LMXB}$ scales roughly with the encounter frequency $\Gamma = \rho_c^2 r_c^3 / \sigma$, where r_c is the core radius (Verbunt & Hut 1987).

The observations of LMXBs in our galaxy suffer from low number statistics–only 12 clusters have LMXBs–so attempts to understand the LMXB formation rate from them have difficul-ties (e.g. Bregman et al. 2006). Observations of qLMXBs in our galaxy also suffer from low number statistics, as only two dozen clusters have been observed with Chandra sufficiently to iden-tify most qLMXBs. Pooley & Hut (2006) and Heinke et al. (2006) study overlapping samples of clusters using different assumptions. Their estimates of the density dependence of qLMXB production for the case of no metallicity dependence also overlap, suggest-

Figure 4. The collision numbers γ and numbers of LMXBs in simulated clusters. The solid line corresponds to $n_{\mathrm{LMXB}} = (2.7 \pm 6) + 0.028\gamma$. The error bars correspond to the scatter in our simulations.

ing a density dependence larger than suggested by Γ, but with large errors. Heinke et al. (2006) also investigate the possibility of metallicity dependence, which decreases the required density dependence.

Observations of LMXBs in globular clusters of other galaxies do not suffer from low statistics, and thus have clearly demonstrated a strong dependence of LMXB production on metallicity (Kundu et al. 2002, 2007). Analyses by Jordán et al. (2004) and Sivakoff et al. (2006) both find that LMXB production has a density dependence lower than Γ. However, it may not be possible to determine the structural properties of extragalactic globular clusters with high accuracy, so uncertainty in the density dependence remains.

On Fig. 4 we demonstrate how the specific number of LMXBs $n_{\mathrm{LMXB}} = N_{\mathrm{LMXB}}/M$ depends on the specific collision frequency $\gamma = \Gamma/M$, taken per units of $10^6 \ M_\odot$, as in Pooley & Hut (2006). It can be clearly seen, that for the case when only density of the clusters is varied, n_{LMXB} depends linearly on γ, however all the other models create a scatter. We urge therefore not to apply blindly the dependence of the number of LMXBs on Γ for the observed clusters and not to search for an unique power law; the scatter in γ in the observed GCs could easily be explained by the variance in other dynamical properties. If one assumes that in the observed sample of GCs the density increase is likely to be accompanied with the increases of the cluster mass, and, accordingly, t_{rh} and σ, then we expect from our results that the power dependence of n_{LMXB} with γ is a bit less than one and close to the value of 0.8 as in Sivakoff et al. (2006), where metallicity effects are separated from dynamical effects.

Even though a typical cluster contains 1 or 2 NS-MS LMXBs, there is only $\sim 10 - 20$ per cent chance that those LMXBs will be bright and persistent, and only in the case of a metal-rich cluster. The probability to contain a bright persistent UCXBs is no more than 10 per cent and does not depend strongly on the metallicity. Overall, there is at best 30 per cent chance to contain a bright

LMXBs in a typical metal-rich cluster and 10 per cent chance – in a metal-poor cluster. This may explain the observed ratio between the bright LMXBs in metal-poor and metal-rich clusters. However, to confirm that, it is necessary to have observational statistics on qLMXBs in both metal-poor and metal-rich clusters – if the explanation above is correct, the number of qLMXbs will not show the dependence on the metallicity. Considering rich Galactic globular clusters, we find that our formation rate of UCXBs at 11 Gyr in Terzan 5 is about 10 per Gyr and ~ 5 per Gyr in Tuc 47 (see Fig. 3). Since $\tau_{\mathrm{UCXB}} \sim 10^8$ yr, this is in agreement with the presence of one bright UCXB in Terzan 5 and no bright UCXB detected in 47 Tuc.

To compare the entire population of UCXBs in GCs with the results of our simulations, we integrated through the whole sample of galactic globular clusters, using data for velocities from Gnedin et al. (2002) and for other quantities from Harris (1996). For these calculation, we used the formation rates shown in the Table 6 and assumed that an UCXB will be bright only 10^8 yr. As a result, the integral value of bright UCXBs in our Galaxy is 7.5, which is pretty close to the observed number of 4 to 10 UCXBs in GCs. The clusters that are most likely to contain UCXBs overlap very well with the clusters where those UCXBs are observed: NGC 1851 and NGC 7078 each have a probability to contain an UCXB > 20 per cent. NGC 6712 is known to have been heavily tidally stripped, so its current cluster conditions do not reflect the conditions that produced its UCXB (see Ivanova et al. 2005). Core-collapsed clusters are not properly modeled by our code, so our failure to predict UCXBs in NGC 6624 and NGC 6652 (a likely UCXB) is not meaningful. Other clusters that have a > 20 per cent chance to contain a UCXB include 47 Tuc, Terzan 5, NGC 6266, NGC 6388, NGC 6440, NGC 6441, NGC 6517, and NGC 6715 (M54). Those clusters have not been shown to contain bright UCXBs, but they generally contain numerous quiescent LMXBs (some of which may be UCXBs) and MSPs (some of which may be products of UCXB evolution). Overall, it seems that physical collisions are able to produce UCBXs in numbers comparable to observed in our Galaxy.

It is more difficult to make a similar comparison for NS-MS LMXBs, as the life-time at the bright stage is much less certain. We identified those clusters that are predicted to contain 5 or more NS-MS LMXBs, and most of those LMXBs will be at quiescence. In the whole GCs population we expect to have about 180 qLMXBs formed through tidal captures and binary exchanges. We note that since our numbers for core-collapse clusters are at the lower limit, the real number of qLMXBs is expected to be higher. The list of the clusters is the same 10 clusters as noted above for UCXBs: 47 Tuc, Terzan 5, NGC 1851, NGC 6266, NGC 6388, NGC 6440, NGC 6441, NGC 6517, M 54, NGC 7078. 5 of them, 47 Tuc, Terzan 5, NGC 6266, NGC 6388 and NGC 6440 are known to contain 5 or more qLMXBs (Heinke et al. 2003, Cohn et al. 2007 in prep). NGC 6441 and NGC 7078 contain bright LMXBs with MS donors (Verbunt & Lewin 2004). We cannot make clear predictions for the core-collapsed, heavily reddened clusters Terzan 1, Liller 1, and Terzan 6 because we do not model dynamical evolution of clusters experiencing core collapse. We note that if AIC binaries contribute to the LMXBs formation, the numbers will go up, although not strongly as the characteristic MT time in this case is shorter than in the case of an average dynamically formed NS-MS binary.

For extragalactic globular clusters, it was shown that the observed luminosity functions can be explained by constant birth of UCXB binaries (Bildsten & Deloye 2004), at the average rate of 10 per Gyr per 200,000 $M_\odot$. Even though we indeed obtained almost

Table 9. Types of pulsars, at 11 Gyr, Terzan 5.

	Halo		Core	
	Total	Binary	Total	Binary
All pulsars				
All	55.2 ± 6.8	38.0 ± 3.0	201 ± 11	56.5 ± 8.9
MT	36.7 ± 5.7	35.3 ± 4.9	109 ± 12	49.2 ± 7.9
CE	2.1 ± 2.2	1.9 ± 2.2	6.2 ± 2.9	1.5 ± 1.1
DCE	0.0 ± 0.0	0.0 ± 0.0	2.3 ± 1.6	2.3 ± 1.6
Merg	16.4 ± 3.9	0.8 ± 0.8	83.5 ± 7.3	3.6 ± 1.2
Core Collapse				
All	6.6 ± 0.9	0.0 ± 0.0	4.5 ± 1.4	0.8 ± 0.4
MT	0.0 ± 0.0	0.0 ± 0.0	0.9 ± 1.2	0.2 ± 0.4
CE	0.0 ± 0.0	0.0 ± 0.0	0.0 ± 0.0	0.0 ± 0.0
DCE	0.0 ± 0.0	0.0 ± 0.0	0.2 ± 0.4	0.2 ± 0.4
Merg	6.6 ± 0.9	0.0 ± 0.0	3.4 ± 1.6	0.4 ± 0.5
ECS				
All	10.4 ± 1.8	3.8 ± 1.6	80.9 ± 9.1	11.9 ± 3.0
MT	1.3 ± 0.8	1.1 ± 0.8	20.6 ± 3.9	7.2 ± 2.2
CE	2.1 ± 2.2	1.9 ± 2.2	4.3 ± 2.7	1.3 ± 0.8
DCE	0.0 ± 0.0	0.0 ± 0.0	1.5 ± 1.1	1.5 ± 1.1
Merg	7.0 ± 2.6	0.8 ± 0.8	54.4 ± 2.9	1.9 ± 1.3
AIC				
All	36.5 ± 5.6	33.1 ± 4.3	89.2 ± 10	40.3 ± 6.9
MT	34.2 ± 4.8	33.1 ± 4.3	82.4 ± 10	39.9 ± 7.3
CE	0.0 ± 0.0	0.0 ± 0.0	0.0 ± 0.0	0.0 ± 0.0
DCE	0.0 ± 0.0	0.0 ± 0.0	0.2 ± 0.4	0.2 ± 0.4
Merg	2.3 ± 0.8	0.0 ± 0.0	6.6 ± 0.9	0.2 ± 0.4
MIC+CIC				
All	1.7 ± 1.4	1.1 ± 1.2	26.3 ± 4.4	3.6 ± 2.4
MT	1.1 ± 1.2	1.1 ± 1.2	4.9 ± 3.5	1.9 ± 1.3
CE	0.0 ± 0.0	0.0 ± 0.0	1.9 ± 1.3	0.2 ± 0.4
DCE	0.0 ± 0.0	0.0 ± 0.0	0.4 ± 0.5	0.4 ± 0.5
Merg	0.6 ± 0.5	0.0 ± 0.0	19.1 ± 4.6	1.1 ± 1.2

The number of pulsars that are retained in the halo and in the core of the model of Terzan 5. Shown separately pulsars that were formed via CC, ECS, AIC or MIC, and that gained mass through different mechanism (a mass transfer, during a common envelope or as a result of a merger).

Table 10. Types of pulsars at 11 Gyr, 47 Tuc.

	Halo		Core	
	Total	Binary	Total	Binary
All pulsars				
All	140 ± 15	79.1 ± 3.9	177 ± 16	75.0 ± 13
MT	71.8 ± 5.7	71.4 ± 5.3	92.6 ± 20	59.1 ± 15
CE	9.4 ± 4.2	7.8 ± 3.6	6.9 ± 3.1	3.3 ± 2.7
DCE	0.0 ± 0.0	0.0 ± 0.0	8.2 ± 2.9	8.2 ± 2.9
Merg	59.1 ± 11	0.0 ± 0.0	69.3 ± 5.1	4.5 ± 2.2
Core Collapse				
All	22.4 ± 8.8	1.6 ± 2.7	6.9 ± 6.0	2.0 ± 2.0
MT	1.6 ± 2.7	1.6 ± 2.7	0.8 ± 1.1	0.4 ± 0.9
CE	0.8 ± 1.1	0.0 ± 0.0	0.0 ± 0.0	0.0 ± 0.0
DCE	0.0 ± 0.0	0.0 ± 0.0	0.8 ± 1.1	0.8 ± 1.1
Merg	20.0 ± 6.0	0.0 ± 0.0	5.3 ± 5.5	0.8 ± 1.1
ECS				
All	33.4 ± 6.2	8.2 ± 4.3	77.9 ± 14	22.0 ± 11
MT	0.4 ± 0.9	0.4 ± 0.9	15.5 ± 4.5	9.8 ± 5.8
CE	8.6 ± 3.6	7.8 ± 3.6	6.5 ± 2.7	3.3 ± 2.7
DCE	0.0 ± 0.0	0.0 ± 0.0	5.7 ± 1.7	5.7 ± 1.7
Merg	24.5 ± 4.8	0.0 ± 0.0	50.2 ± 9.6	3.3 ± 2.3
AIC				
All	84.4 ± 4.5	69.3 ± 6.7	85.2 ± 21	48.9 ± 15
MT	69.7 ± 7.2	69.3 ± 6.7	75.4 ± 18	48.5 ± 14
CE	0.0 ± 0.0	0.0 ± 0.0	0.4 ± 0.9	0.0 ± 0.0
DCE	0.0 ± 0.0	0.0 ± 0.0	0.4 ± 0.9	0.4 ± 0.9
Merg	14.7 ± 4.6	0.0 ± 0.0	9.0 ± 4.9	0.0 ± 0.0
MIC+CIC				
All	0.0 ± 0.0	0.0 ± 0.0	6.9 ± 2.3	2.0 ± 2.0
MT	0.0 ± 0.0	0.0 ± 0.0	0.8 ± 1.8	0.4 ± 0.9
CE	0.0 ± 0.0	0.0 ± 0.0	0.0 ± 0.0	0.0 ± 0.0
DCE	0.0 ± 0.0	0.0 ± 0.0	1.2 ± 1.8	1.2 ± 1.8
Merg	0.0 ± 0.0	0.0 ± 0.0	4.9 ± 1.1	0.4 ± 0.9

Notations are as in Table 9, but for the model of 47 Tuc.

constant birth for such binaries, our rates are significantly lower (it is one per Gyr for 200,000 $M_\odot$ in a typical "dense" cluster). A 10 times higher UCXB formation rate must result in the presence of as many as 10 bright persistent LMXBs in Terzan 5. There is still a possibility that the mass function of GCs in ellipticals differs from that in our galaxy. Then more massive GCs will produce on overall more UCXBs, however the mass of such clusters then must be 10 times more than the mass of Terzan 5. In addition, as we do not find any difference in the number of formed UCXBs binaries in metal-poor and metal-rich populations, our simulations do not support the idea that most X-ray binaries in extragalactic GCs are UCXBs.

7 MILLISECOND PULSARS

In the Table 8 we show the number of pulsars that are formed in our simulations (see also §2.3). In this table, we count as pulsars all NSs that gained more than 0.01 $M_\odot$ after their formation, through all the possible mechanisms of mass gain (mass transfer, common envelope accretion and during mergers or physical collisions). There are three most important facts that can be seen from the table: (i) the numbers of ejected and retained pulsars are comparable; (ii) almost all NSs in binaries are pulsars; (iii) the numbers of produced pulsars are very large, more than several times the number of detected pulsars in specific galactic clusters (compare 320 MSPs in simulations vs 22 detected MSPs for 47 Tuc or 250 MSPs in simulation vs 33 detected MSPs in Terzan 5).

The latter shows that a direct comparison of numbers of NSs that gained a mass with the observed numbers of MSPs fails, unless the detection probability is only about 10 per cent (however this should be at least 33 per cent and may be even close to one, see Heinke et al. 2005). The alternative is that we produce and retain in simulations much more NSs than are retained in real GCs. In this case we could not explain with our simulations the observable number of LMXBs. On the other hand, as we discussed in §2.3, the detectability of a MSP might depend on its formation history. Those NSs that were formed through AIC or MIC are likely to have high magnetic fields, and, accordingly, their lifetimes as MSPs can be only $10^7 - 10^8$ years (see Eq. 8), meaning that they can be seen as MSPs only if they experienced MT during the last ~ 0.1 Gyr or less. In addition, it is not certain that all the mechanisms for mass gain lead to NS spin-up. Physical collisions resulting in mergers are quite poorly understood, for example.

Let us also review the expected differences between the observed periods of short-period bMSPs with very low-mass companions and the modeled periods. Using a standard mass-radius relation for WDs during the MT evolution of a NS-WD binary, formed binaries have the period several times smaller than in observed binary MSPs (bMSPs) with companions of similar masses. It has been shown that even the consideration of more realistic WD

Table 8. Pulsars and their location at 11 Gyr.

model	Halo			Core			Ejected		
	All psrs	Bin psrs	NS-bin	All psrs	Bin psrs	NS-bin	All psrs	Bin psrs	NS-bin
standard	24.8 ± 3.5	16.9 ± 3.3	19.5 ± 3.1	39.0 ± 4.4	17.0 ± 2.6	19.9 ± 2.8	103 ± 9.1	34.6 ± 5.1	41.6 ± 6.2
metal-poor	23.3 ± 4.8	17.6 ± 4.0	20.7 ± 4.1	42.4 ± 5.6	19.2 ± 2.2	23.3 ± 2.6	125 ± 10.0	33.9 ± 4.2	51.9 ± 11
high-den	41.7 ± 10	31.3 ± 5.1	35.3 ± 5.5	97.5 ± 5.1	21.8 ± 4.5	23.2 ± 4.6	223 ± 4.7	138 ± 12	159 ± 16
med-den	11.8 ± 3.4	11.6 ± 3.7	15.0 ± 3.3	16.2 ± 2.9	14.3 ± 3.2	19.0 ± 4.3	26.6 ± 2.3	26.3 ± 2.3	62.5 ± 36
low-den	21.8 ± 1.2	15.2 ± 1.5	17.7 ± 2.4	18.4 ± 2.6	13.1 ± 1.5	17.3 ± 2.2	85.5 ± 9.2	25.3 ± 5.4	42.9 ± 15
low-σ	9.1 ± 3.7	5.3 ± 2.1	6.4 ± 1.8	14.1 ± 2.8	3.6 ± 1.7	4.6 ± 2.3	167 ± 9.3	86.3 ± 7.9	106 ± 14
long-$t_{\rm rh}$	30.2 ± 5.0	21.6 ± 4.1	25.9 ± 5.0	17.1 ± 2.1	7.5 ± 3.2	8.6 ± 3.2	93.0 ± 9.7	29.9 ± 3.7	55.8 ± 24
BF05	15.6 ± 3.9	10.2 ± 3.5	12.4 ± 2.9	29.5 ± 6.3	13.6 ± 2.8	15.8 ± 2.6	67.1 ± 7.6	23.0 ± 4.6	38.0 ± 13
fast-MB	24.5 ± 3.6	16.0 ± 3.9	18.3 ± 4.3	45.4 ± 4.3	18.6 ± 2.7	22.2 ± 2.5	107 ± 10	36.9 ± 4.6	50.3 ± 9.9
CE-reduced	7.8 ± 1.1	3.2 ± 1.5	4.9 ± 2.5	30.7 ± 3.0	12.0 ± 2.4	15.3 ± 2.9	17.0 ± 1.4	6.8 ± 2.4	18.7 ± 11
oldkicks	8.9 ± 3.7	0.3 ± 0.7	0.3 ± 0.7	10.2 ± 3.2	2.1 ± 1.6	2.3 ± 1.8	67.0 ± 4.7	4.4 ± 2.3	12.4 ± 4.6
47 Tuc	140 ± 15	79.1 ± 3.9	104 ± 9.1	177 ± 16	75.0 ± 13	85.6 ± 15	403 ± 15	104 ± 10	136 ± 11
Terzan 5	55.2 ± 6.8	38.0 ± 3.0	40.3 ± 2.4	201 ± 11	56.5 ± 8.9	64.1 ± 9.1	224 ± 13	139 ± 11	178 ± 32

The number of pulsars that are retained in the halo or core of the cluster, as well as the number of ejected pulsars. As a pulsar we define here a NS that gained mass $> 0.01 M_\odot$ after its formation. "All psrs" - the number of all pulsras, "Bin psrs" - the number of binary pulsars and "NS-bin" - the number of all NSs in binaries, provided for the comparison. For all GC models, except 47 Tuc and Terzan 5, the numbers are scaled per 200 000 $M_\odot$ stellar population mass at the age of 11 Gyr; for 47 Tuc the numbers are given per its total mass taken as 10^6 $M_\odot$, for Terzan 5 - per 370 000 $M_\odot$.

Table 11. "Observable" pulsars at 11 Gyr.

model			low-B							high-B
	All psrs	Single				Binary				Total
Companion			BD	WD		MS	He WD	heavy WD		
$M_{\rm c}$		$< 0.01 M_\odot$					$\lesssim 0.5 M_\odot$	$\gtrsim 0.5 M_\odot$		
Period			< 0.1d	< 0.1d	> 10d		$0.1 \div 10$d	$0.1 \div 10$d		
standard	3.5 ± 1.4	0.9 ± 0.7	0.6 ± 0.8	0.2 ± 0.3	0.9 ± 0.9	0.5 ± 0.5	0.2 ± 0.3	0.7 ± 1.1	0.0 ± 0.0	34.6 ± 6.2
metal-poor	2.6 ± 1.1	1.0 ± 0.7	0.3 ± 0.4	0.0 ± 0.0	0.5 ± 0.4	0.3 ± 0.4	0.0 ± 0.0	0.8 ± 0.6	0.0 ± 0.0	41.8 ± 5.7
high-den	11.8 ± 2.1	6.0 ± 1.5	1.2 ± 1.5	0.9 ± 1.1	1.8 ± 1.4	0.0 ± 0.0	1.1 ± 1.4	2.3 ± 0.5	0.4 ± 0.5	68.0 ± 6.0
med-den	0.6 ± 0.7	0.3 ± 0.4	0.0 ± 0.0	0.0 ± 0.0	0.0 ± 0.0	0.0 ± 0.0	0.2 ± 0.4	0.2 ± 0.4	0.0 ± 0.0	27.4 ± 4.7
low-den	0.0 ± 0.0	0.0 ± 0.0	0.0 ± 0.0	0.0 ± 0.0	0.0 ± 0.0	0.0 ± 0.0	0.0 ± 0.0	0.0 ± 0.0	0.0 ± 0.0	24.1 ± 3.9
low-σ	1.7 ± 1.2	1.0 ± 1.1	0.2 ± 0.4	0.2 ± 0.4	0.2 ± 0.4	0.2 ± 0.4	0.2 ± 0.4	0.2 ± 0.4	0.0 ± 0.0	9.3 ± 3.4
long-$t_{\rm rh}$	0.6 ± 0.7	0.0 ± 0.0	0.2 ± 0.4	0.2 ± 0.4	0.2 ± 0.4	0.2 ± 0.4	0.0 ± 0.0	0.2 ± 0.4	0.0 ± 0.0	27.3 ± 5.8
BF05	2.5 ± 0.8	0.4 ± 0.7	0.9 ± 0.6	0.1 ± 0.3	1.0 ± 0.4	0.4 ± 0.4	0.1 ± 0.3	0.3 ± 0.7	0.0 ± 0.0	22.8 ± 5.2
fast-MB	6.1 ± 1.2	1.5 ± 0.9	1.0 ± 0.9	1.0 ± 0.7	1.1 ± 0.7	0.3 ± 0.4	1.1 ± 0.7	1.5 ± 0.9	0.0 ± 0.0	35.3 ± 1.5
CE-reduced	3.1 ± 1.8	1.0 ± 1.5	0.6 ± 0.7	0.2 ± 0.4	1.0 ± 0.4	0.3 ± 0.4	0.2 ± 0.4	0.5 ± 0.7	0.0 ± 0.0	14.0 ± 4.8
oldkicks	1.5 ± 1.5	0.0 ± 0.0	0.0 ± 0.0	0.3 ± 0.4	0.0 ± 0.0	0.8 ± 0.8	0.5 ± 0.4	0.3 ± 0.7	0.0 ± 0.0	0.0 ± 0.0
47 Tuc	22.4 ± 4.5	6.1 ± 3.8	3.3 ± 2.3	1.6 ± 1.7	4.5 ± 3.9	2.9 ± 3.4	1.2 ± 1.8	6.1 ± 2.0	0.4 ± 0.9	149 ± 21
Terzan 5	22.7 ± 3.2	14.7 ± 3.0	2.5 ± 1.6	0.9 ± 1.2	4.5 ± 1.0	0.4 ± 0.5	0.8 ± 0.8	1.5 ± 0.8	0.4 ± 0.5	125 ± 8.7

The numbers of pulsars that can be detected in a GC. Assumed that in order to become a MSP, a NS gained mass only via MT or DCE. Low-B pulsars are the pulsars that were formed via CC or ECS and high-B pulsars are the pulsars that were formed via AIC, MIC or CIC. For this table, we count high-B pulsars which were formed less than 10^8 years ago as low-B pulsars, as they did not yet spun down. Mass-transferring NS-MS binaries where a MS star is $\gtrsim 0.2 M_\odot$ are excluded as appearing as LMXBs/qLMXBs. Companion shows the type of the companion. $M_{\rm c}$ is the mass of the companion and period is the orbital period. For all GC models, except 47 Tuc and Terzan 5, the numbers are scaled per 200 000 $M_\odot$ stellar population mass at the age of 11 Gyr; for 47 Tuc the numbers are given per its total mass taken as 10^6 $M_\odot$, for Terzan 5 - per 370 000 $M_\odot$.

model does not change the result strongly – hotter donors don't, by themselves, give the periods one needs to explain the short-period bMSPs (Deloye & Bildsten 2003). If a mass-losing companion is a WD, some special processes must be involved – e.g., tidal heating of a WD during the MT (Rasio et al. 2000). In that case, it is not possible to predict well their periods during the MT or at its end.

Speaking about the end of the MT we must mention that there is no special external mechanism that would interrupt the MT from a degenerate donor. As a result, the MT continues uninterrupted and within the Hubble time the companion mass can be as small as under 0.01 $M_\odot$. No observed bMSPs have been shown to have such low-mass companions, in globular clusters or the field. There-

fore some MT interruption mechanism must exist and it is likely that in our simulations we keep too many of bMSPs with low-mass companions.

If the MT occurred in a NS-MS binary, then the resulting binary will have at short periods a degenerate hydrogen companion. Such a companion is bigger than a regular WD and, accordingly, the binary period of a formed bMSP is larger and explains the observed ones better.

In order to understand the modeled population better, we make the comparison of our results with the observations of 47 Tuc and Terzan 5. On Figs. 5 and 6 we compare the populations of observed and modeled binary MSPs in 47 Tucanae and Terzan 5. We use all

simulated models for those clusters, and, as a result, shown modeled populations are about 2 times larger than in the observed cluster for 47 Tuc and 5 times larger than in the case of Terzan 5. There are three panels for each cluster, each panel shows the observed population and the simulated population where pulsars gained mass via different mechanism (MT, CE or dynamical common envelope (DCE) during a physical collision with a giant, and as a result of the merger). For most of the observed MSPs, the companion masses are calculated assuming a pulsar mass of 1.35 solar masses and an inclination of 60 degrees[4], leading to an uncertainty in the direct comparison of observations and simulations. In Tables 9 and 10 we show the data for MSPs in 47 Tucanae and Terzan 5 distinguishing them by their formation mechanism and by the process through which they acquired mass after the NS formation.

Primordial bMPS. This population is present on the panels that show pulsars that gained mass via MT and via CE. The first population (MT) is characterized by rather large period and small companion masses. A representative of such population was detected in Terzan 5, but was not in 47 Tuc. Quite likely that this due to a smaller total number of bMSPs in 47 Tuc.

The second population, characterized by a companion mass around $1M_\odot$ is however undetected in both clusters. A typical progenitor is an initially wide binary with two companions of rather similar masses from 6 to 10 $M_\odot$. Most of the primordial bMPSs are located in the halo. There are several possible explanations for these bMSPs to not be present in real clusters:

• CE does not lead to the NS spun up and MSPs formation;
• as NSs in those bMSPs are mainly post-ECS or post-AIC (see Tables 9 and 10) – possibly, kicks must be higher and so such systems would rather be destroyed than evolve via CE;
• CE prescription adopted in our code ($\alpha_{CE}\lambda = 1$) can not produce realistic results;
• our mass segregation does not work properly for progenitors of this bMSPs – if they would segregate in the code faster, then they would be destroyed and will not produce bMSPs.

Physical collisions. This population is present on two panels on Figs. 5 and 6 – among the NSs that gained mass via MT and via DCE. In the first case, bMSPs still continue MT and appear as UCXBs. As we mentioned before, we (i) don't have a theoretically predicted mechanism to stop the MT and (ii) such binaries do not reach periods comparable to observed ones. Binary encounters appeared to be inefficient in breaking those systems, and as a result they are present in large numbers in both clusters, including those bMSPs that have extremely low-mass companions ($\lesssim 0.01M_\odot$) and were not detected in Galactic GCs. It does not mean however that we overproduce low-mass companions bMSPs which are UCXBs descendants – if in nature a WD is blown up, then the MT rate, which is mainly driven by gravitational waves radiation is decreasing. An NS-WD system will live longer, but will have a bigger period and its companion will have a bigger mass for a longer time than in our simulations.

The rate of PCs has the largest variation between the five simulated models in the case of Terzan 5. For this cluster, we produce rather small number of binary pulsars with low-mass companions $0.01M_\odot \lesssim M_c \lesssim 0.1M_\odot$ (as a fraction of the total bMSPs population), this fraction is smaller than in the case of 47 Tucanae and it seems to coincide with the observations.

The population of bMSPs where a pulsar has been spun-up via DCE agrees nicely with the observations of eccentric pulsars.

Tidal captures. This population is present on all the panels as the spin-up occurred before the system was formed. This channel is the best to explain the observed non-eccentric bMSPs with periods less than a day.

Binary exchanges lead to the formation of an eccentric population with periods extending to 1000 days and companion masses up to above the turn-off mass (blue stragglers); most of the companions are non-degenerate. The top panels on Figs. 5 and 6 show those of BE bMSPs which still undergone MT. When a companion mass is above $\sim 0.2M_\odot$, the MT rate in these systems is high and they will rather appear as LMXBs. Those of the bMSPS which are presumably spun-up via mergers during a previous dynamical interaction, have companions too massive and periods too large, compared to the observed populations. It is likely therefore that mergers do not lead to a NS spun-up. We note that we do not dynamically form binaries that would undergo a stable MT with a giant and would be non-eccentric having large periods. Such systems only come from the primordial population.

We conclude that bMSPs produced in our simulations, but not present, or not detectable, in GCs include:

• Primordial bMSPs where a NS gained mass via CE
• bMSPs where a NS gained mass via merger
• Mass transferring NS-MS systems with MS mass $\gtrsim 0.2M_\odot$, as they most likely are seen only as LMXBs/qLMXBs
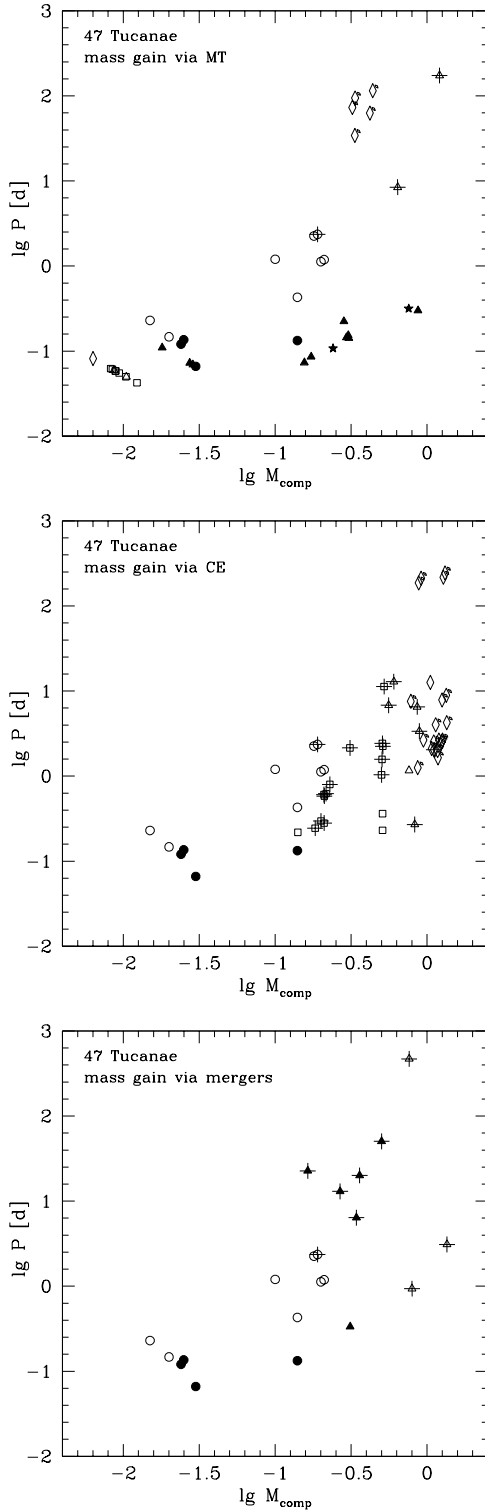• Systems where a NS was formed via AIC/MIC more than 10^8 yr ago

Excluding these bMSPs from our statistics, we find that the firm lowest estimate for the numbers of produced MSPs are 23 ± 3 MSPs in Terzan 5 and 22 ± 5 in 47 Tuc. This estimate is close to the observations – 22 detected MSPs in 47 Tuc and 33 in Terzan 5. The binary population of MSPs is $1/2 - 1/3$ of all MSPs.

We predict that the fraction of single pulsars is higher in Terzan 5 than in 47 Tuc, as observed. The origin of isolated MSPs depends on the cluster dynamical properties. For example, in our standard model, about half of isolated MSPs were formed in a result of an evolutionary merger at the end of the MT from a MS companion, and another half lost their companion as a result of a binary encounter. Most such binary encounters occurred in systems where a NS was spun-up during MT from a giant, and had a WD companion just before it become single. In the case of 47 Tuc, very few isolated pulsars were formed in a result of an evolutionary merger at the end of the MT. Most lost their companion as a result of a binary encounter, where in half of the cases the companion before the binary destruction was a low-mass WD or MS star at the end of their MT sequence.
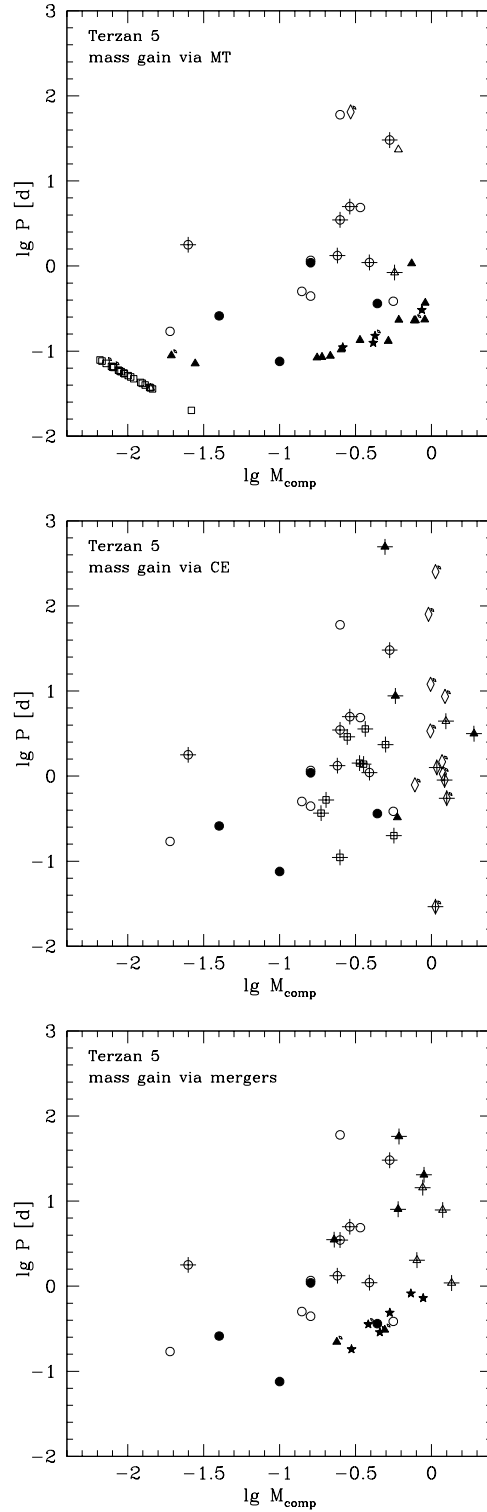
Spatially, MSPs are more likely to be located where they were formed – mostly in the core. Less than a third are located in the halo – primordial or recoiled. Fraction of recoiled MSPs is increasing with v_{rec} decrease. Roughly half of observed pulsars are found outside their cluster core radius (Camilo & Rasio 2005), but the radial distribution of most pulsars is exactly as expected for a population that is produced in or around the core (Grindlay et al. 2002; Heinke et al. 2005), with the exception of a few, likely ejected, pulsars in M15 and NGC 6752 (e.g. Colpi et al. 2002).

It is possible that not all of the AIC MSPs posses high magnetic field, and therefore may contribute both to the total number of the pulsars as well as to the binary fraction of MSPs and to their location (see Tables 9 and 10). The creation rate of high-magnetic field AIC MSPs, at the age of 11 Gyr, is about 10 per Gyr in Terzan

---

[4] See http://www2.naic.edu~pfreire/GCpsr.html

Figure 5. Binary MSPs in 47 Tucanae: observed and modeled populations: circles – observed, stars – formed via TC, squares – formed via PC, triangles – formed via binary encounters and diamonds – "primordial" binary MSPs. Filled symbols represent binary MSPs with non-WD companions; in the case of observed systems filled symbols represent eclipsing bMSPs. Crosses mark eccentric bMSPs ($e > 0.05$), small rotated diamonds mark bMSPs in the halo. Modeled population represents accumulative results from 5 models and corresponds to 2 times bigger stellar population than in 47 Tucanae.

Figure 6. Binary MSPs in Terzan 5: observed (circles) and modeled (triangles) populations, symbols are as on Fig. 5. Modeled population represents accumulative results from 5 models and corresponds to 5 times bigger stellar population than in Terzan 5.

5 and 47 Tuc. This leads to the presence probability of a high-magnetic field MSPs ($B \lesssim 10^{12}$-gauss) with a period $\geqslant 100$ ms less than 1 per cent, and for $B \lesssim 10^{11}$-gauss, it is about 15 per cent (see eq. 8). One pulsar in Terzan 5 (J1748-2446) has P=80 ms Ransom et al. (2005), and might be a high-field system produced by AIC. Absence of slow-period MSPs in 47 Tucanae suggests that the magnetic field in formed AIC NSs is most likely be at a higher end, $\gtrsim 10^{12}$-gauss.

We also compared the predictions of the types of pulsars generated in our models to the observations of all known up-to-date globular cluster pulsars (see Table 12). We divide the clusters containing MSPs with known properties into categories corresponding to the central densities used in the models: High-density ($\rho_c > 5.35$; also containing other core-collapsed): NGC 1851, NGC 6342, NGC 6397, NGC 6522, NGC 6544, NGC 6624, M15, M30. Terzan-5-like ($5.05 < \rho_c < 5.35$): NGC 6266, Terzan 5, NGC 6440, NGC 6441. 47Tuc-like ($4.6 < \rho_c < 5.05$): 47 Tuc, NGC 6626, NGC 6752. Standard ($3.8 < \rho_c < 4.6$): M5, M4, NGC 6760. Medium-density ($2.8 < \rho_c < 3.8$): M53, M3, M13, NGC 6539, NGC 6749, M71. No pulsars have been found to inhabit low-density clusters yet.

The column "All pulsars" indicates the total number of pulsars used in that category; other columns refer to fractions of that number. The total numbers of pulsars cannot be directly compared to the numbers of pulsars in the model, but the fractions of pulsar system types can be compared. Field systems include all field pulsars with $P < 100$ ms and $B < 5 \times 10^{10}$ G. BD refers to brown dwarf systems; $M_{comp} < 0.07\ M_\odot$. MS identifies likely main-sequence companions, identified by being eclipsing systems with $M_{comp} > 0.07\ M_\odot$ (Freire 2005). He WDs refer to all non-eclipsing companions with $0.07 < M < 0.5\ M_\odot$. C/O WDs were all MSPs with companion masses $\gtrsim 0.5\ M_\odot$, unless the companion is known to be a NS. "> 10 d" refers to that subset of all MSPs with orbital periods longer than 10 days. High-B pulsars are taken to be MSPs with spin-period $P \gtrsim 100$ ms in globular clusters, which may have an unusual formation mechanism (Lyne et al. 1996). We compare the observed systems to our model systems. Note that for our predicted numbers of high-B systems we consider all high-B pulsars that were spun-up within last 3 Gyr and divide this number by a factor of 30 to account for their shorter lifetimes.

Several clear trends with the central density of globular clusters can be seen in the observations. Single MSPs rise smoothly from a rate of 0.25 of all MSPs in the field, to 0.6 of all MSPs in clusters. This is well-described by our model, suggesting that the formation of single MSPs may be reasonably understood (again, please note a large scatter, especially for "med-den" models, where very few pulsars were formed). The formation of MSPs with "brown dwarf" companions, with very low masses, exhibit a complicated density dependence, with few in the field, a quarter of all MSPs in medium-density clusters, and declining fractions in higher density clusters. This indicates that their formation requires a high density environment, but also suggests that their binary evolution can be disrupted in high density conditions. A similar trend can bee seen in our results, with the exception for "med-den", possibly due to small number statistics. The production of MSPs with main-sequence companions and of high-B MSPs are sharply dependent on the central density of the cluster, in agreement with the suggestions by Freire (2005) and Lyne et al. (1996) that their production requires multiple binary interactions, and direct impact of NSs with other stars, respectively. Overall, almost all our numbers are in agreement with the observations if the numerical scatter is taken into account.

8 DOUBLE NEUTRON STARS IN GCS

As it was predicted in §5.1, we did not find an efficient primordial double neutron star formation. In all our simulations – 70 cluster models or $2 \times 10^7 M_\odot$ of stellar population evolved in different clusters, only 3 primordial DNSs has been formed. In all three systems, NSs were formed via ECS and none of the systems has merged within a Hubble time.

Let us estimate the rate of dynamical DNSs formation. The characteristic time for a single NS to have an encounter with a NS-binary can be estimated using the eq. 10. A binary companion in a NS-binary is usually less massive than a NS. If an exchange occurs, the binary separation in a formed post-exchange binary a is larger than the binary separation a_0 in the pre-exchange binary, $a \sim a_0 m_{NS}/m_2$, where m_2 is the mass of the replaced companion (Heggie et al. 1996). Binary eccentricities in hard binaries follow a thermal distribution, with an average eccentricity $e \sim 2/3$ (Heggie 1975). The maximum a that leads to a merger within 11 Gyr, if the post-exchange eccentricity is 2/3, is about $7.5R_\odot$. The maximum mass for a NS-companion before the exchange is about the mass of a turn-off MS star – $0.9M_\odot$. Then the maximum binary separation in a pre-exchange binary that leads to the formation of a merging DNS is $a_0 = 4.8R_\odot$.

From our simulations we find that the relative fraction of NS-binaries in the core $f_{NS-bin,core} = N_{NS-bin,core}/N_{objects,core}$ is 0.175 per cent in the case of a standard model, and 0.6 per cent in the case of Terzan 5. Then the characteristic time for a NS to have an encounter that may lead to the formation of a merging DNS is $\tau_{DNS,m} \approx 5 \times 10^{12}$ Gyr in the case of a standard cluster, in other words, about 500 NSs is required to form one merging DNS within 11 Gyr. This assumed that *every* encounter will lead to the exchange and that *all* NS-binaries have the separation of $\sim 5R_\odot$. In the case of Terzan 5, a chance to form a merging DNS, per NS, is 25 times bigger than in standard cluster – the formation rate is highly dependent on the cluster density, as in power 2, and the number of retained NSs is increasing when escape velocity is increased. However, most of the NS-binaries have bigger binary separations than $\sim 5R_\odot$, and even though encounters are more frequent in this case, they do not lead to the formation of a merging DNS directly, unless subsequent encounters of a formed DNS with other stars in the core will increase DNS's eccentricity, reducing in the result its merging time. In addition, an NS-binary with a $0.9M_\odot$ MS companion, $a = 4.8R_\odot$ and $e \approx 2/3$ will more likely evolve to start the MT and form an LMXB rather than have an encounter with another NS.

Only 14 DNSs have been formed dynamically during 11 Gyr in all our 70 cluster models. As the formation rate of DNSs is highly density dependent, most of those DNSs were formed in cluster models of Terzan 5. Only two of these 14 DNSs merged, another two DNSs merged after 11 Gyr but within the Hubble time 14 Gyr. 5 out of 14 formed DNSs stayed in the cluster for a long time, till 11 Gyr, and 9 remaining were destroyed within a Gyr after their formation.

We note that the formation rate of DNSs is strongly connected to the formation rate of LMXBs, as the main building material of DNSs is NS-binaries that otherwise become LMXBs. As we show in §6, we produce LMXBs in numbers comparable to those observed, but we underestimate the formation rates for core-collapsed clusters. In core-collapsed clusters it is especially clear that our simplified models do not properly treat the cluster dynamics and therefore we cannot be very quantitative about the total number of DNSs that should be produced by all GCs, although only a small fraction of GCs are core-collapsed. We conclude therefore

Table 12. Detected pulsars and simulations.

Cluster	All pulsars	Single	BD	He WD	MS	C/O WD	> 10 d	high-B
High-den model	11.8 ± 2.1	0.51 ± 0.11	0.06 ± 0.05	0.20 ± 0.07	0.10 ± 0.09	0.03 ± 0.04	0.00 ± 0.00	0.03 ± 0.01
All high-den	16	0.63	0	0.06	0.19	0.06	0.06	0.25
Terzan 5 model	22.7 ± 3.2	0.65 ± 0.06	0.11 ± 0.06	0.07 ± 0.04	0.03 ± 0.03	0.03 ± 0.02	0.02 ± 0.02	0.03 ± 0.01
All Ter5	48	0.62	0.10	0.27	0.10	0.06	0.08	0.02
47Tuc model	22.4 ± 4.5	0.27 ± 0.14	0.11 ± 0.13	0.38 ± 0.11	0.06 ± 0.08	0.04 ± 0.08	0.11 ± 0.12	0.02 ± 0.00
All 47Tuc	32	0.47	0.19	0.25	0.09	0	0	0
Standard model	3.5 ± 1.4	0.25 ± 0.20	0.11 ± 0.10	0.32 ± 0.19	0.19 ± 0.31	0.02 ± 0.06	0.13 ± 0.13	0.03 ± 0.02
all stand	9	0.22	0.22	0.56	0	0	0.22	0
Med-den model	0.64 ± 0.67	0.40 ± 0.55	0.00 ± 0.00	0.10 ± 0.22	0.10 ± 0.22	0.00 ± 0.00	0.00 ± 0.00	0.08 ± 0.08
All med-den	8	0.25	0.25	0.50	0	0	0	0
Field	77	0.25	0.04	0.53	0	0.13	0.30	-

Comparisons of the predictions about the nature of cluster pulsar systems with observations of globular cluster pulsars (summarized by Camilo & Rasio (2005), with additions noted at http://www.naic.edu∼pfreire/GCpsr.html as of early 2007). See text (§7) for details.

that if GCs are important for the formation of merging DNSs and provide a significant contribution to the production of short γ-ray bursts in distant galaxies (as it was proposed in Grindlay et al. 2006), such systems can only be produced in core-collapsed clusters, like M15, where such a system is observed (Anderson et al. 1990; Jacoby et al. 2006).

9 SUMMARY

In our study of binaries with neutron stars in globular clusters we considered in detail the problem of formation of LMXBs and MSPs in GCs. With our simulations we predict that most of the retained neutron stars in GCs must come from an electron capture supernova formation channel (c.f. the field, where most NSs are from core-collapse supernovae). A typical GC could contain at present (where the adopted cluster age is 11 Gyr) as many as ~ 220 NSs where about half of them are located in the halo; a massive GC like 47 Tuc could have more than a thousand NSs.

Analyzing encounters with NSs, we find that for NSs located in the core, about half of them formed a binary through an exchange encounter and only a few per cent formed a binary through a physical collision with a giant or via tidal capture. The relative importance of tidal captures to physical collisions increases as the velocity dispersion decreases. Although there are fewer binaries formed though PC and TC than through binary encounters, the production of mass-transferring systems is roughly the same for all the channels. We note as well that there are many physical collisions leading to mergers between NSs and other stars in the core.

Considering LMXB formation, we derived the collision number that seems to be consistent with being linear with the number of LMXBs, although only for the case when only the core density varies. Variations of other GC dynamical properties with a fixed core density lead to large scatter. This explains the observed deviations from a linear dependence between the collision number and the number of LMXBs in non-core-collapsed clusters. We predict that the number of qLMXB may have no dependence on the metallicity, contrary to the number of bright LMXBs.

Our rates of LMXB formation predict 7.5 UCXBs in all galactic GCs, which is consistent with the observed number. For qLMXBs, we expect about 180 systems, which agrees with the range (100-200) estimated from observations (Pooley et al. 2003; Heinke et al. 2003, 2005). From our list of clusters which are expected to have one or more LMXBs (bright or in quiescence) – 47 Tuc, Terzan 5, NGC 1851, NGC 6266, NGC 6388, NGC 6440, NGC 6441, NGC 6517, M54, NGC 7078 – all clusters which have been studied with Chandra (all but NGC 6517) show at least one LMXB or qLMXB. Our results do not support the idea that the observed luminosity function in extragalactic globular clusters is mainly formed by UCXBs.

We find that if all possible channels of NS formation and all possible mechanisms for its spin-up lead to MSP formation, then we overproduce MSPs even though at the same time we need just that many NSs for agreement with the formation rate of LMXBs from observations. We proposed that AIC and MIC produce NSs with very high magnetic fields (such as the MSP NGC 6440A). Such a NS, being spun up, lives only briefly as an MSP. Also, we find that if we assume that a NS would accrete and spin up during a common envelope, we overproduce bMSPs in the cluster halos from primordial binaries of intermediate masses. Such bMSPs would be present in low-density clusters and have not yet been seen. Excluding the systems discussed above, as well as those which are still actively accreting their donor's material and are seen rather as LMXBs, we obtained the number of "detectable" bMSPs. The predicted numbers are in a good agreement with the observations – 22 ± 5 MSPs in 47 Tuc and 23 ± 3 in Terzan 5. The fraction of isolated pulsars is comparable with observations and is bigger in Terzan 5 than in 47 Tuc.

Comparing the population census of our models with the observations of all detected pulsars to date in GCs, we find good agreement for all types of pulsars – single, with brown dwarf companion, with MS companions, with light or heavy WD companions and with large periods.

We do not find very efficient formation rates for double NSs – only a dozen were formed in 70 simulated models. These rates increase with the square of the GC core density. We conclude that DNS formation is most likely to occur in massive, very dense, and preferentially core-collapsed GCs, as suggested by the identification of only one double NS so far, in the core-collapsed GC M15.

In conclusion we outline several important issues that must be addressed for further progress in studies of NSs in globular clusters:

• A common envelope event in primordial binaries of intermediate masses that produce a NS via ECS – whether a NS accretes the material and spun up and what is the common envelope efficiency;

• A result of the mass accretion on a NS after it has experienced a merger – in a binary as a result of unstable mass transfer or during an encounter;

• The final fate of a mass-transferring NS-WD binary – what is the post-MT period or how it lost its companion;

• The dependence of qLMXBs on the cluster metallicity. In particular, if future observations will show that the dependence on the metallicity for qLMXBs follows the one for bright LMXBs, it will most likely indicate that these two types of clusters had difference history of star formation and had different initial mass functions, as was predicted by Grindlay (1993) and is expected by the star formation theory in the case of a dense metal-rich environment (Murray, priv. comm.).

REFERENCES

Anderson S. B., Gorham P. W., Kulkarni S. R., Prince T. A., Wolszczan A., 1990, Nature, 346, 42

Arzoumanian Z., Chernoff D. F., Cordes J. M., 2002, ApJ, 568, 289

Barkat Z., Reiss Y., Rakavy G., 1974, ApJL, 193, L21

Belczynski K., et al. 2007, in prep

Belczynski K., Kalogera V., Bulik T., 2002, ApJ, 572, 407

Belczynski K., Kalogera V., Rasio F. A., Taam R. E., Zezas A., Bulik T., Maccarone T. J., Ivanova N., 2007, ApJS

Belczynski K., Perna R., Bulik T., Kalogera V., Ivanova N., Lamb D. Q., 2006, ApJ, 648, 1110

Bellazzini M., Pasquali A., Federici L., Ferraro F. R., Pecci F. F., 1995, ApJ, 439, 687

Bhattacharya D., van den Heuvel E. P. J., 1991, PhysRep, 203, 1

Biggs J. D., Bailes M., Lyne A. G., Goss W. M., Fruchter A. S., Biggs J. D., 1994, MNRAS, 267, 125

Bildsten L., Deloye C. J., 2004, ApJL, 607, L119

Bregman J. N., Irwin J. A., Seitzer P., Flores M., 2006, ApJ, 640, 282

Brown E. F., Bildsten L., Rutledge R. E., 1998, ApJL, 504, L95

Camilo F., Lorimer D. R., Freire P., Lyne A. G., Manchester R. N., 2000, ApJ, 535, 975

Camilo F., Rasio F. A., 2005, in Rasio F. A., Stairs I. H., eds, ASP Conf. Ser. 328: Binary Radio Pulsars Pulsars in Globular Clusters. pp 147–+

Campana S., Colpi M., Mereghetti S., Stella L., Tavani M., 1998, A&AR, 8, 279

Chapman R., Levan A. J., Wynn G. A., Davies M. B., King A. R., Priddey R. S., Tanvir N. R., 2006, ArXiv Astrophysics e-prints

Clark G. W., 1975, ApJL, 199, L143

Colpi M., Possenti A., Gualandris A., 2002, ApJL, 570, L85

Deloye C. J., Bildsten L., 2003, ApJ, 598, 1217

Dessart L., Burrows A., Ott C., Livne E., Yoon S.-C., Langer N., 2006, ArXiv Astrophysics e-prints

Dieball A., Knigge C., Zurek D. R., Shara M. M., Long K. S., Charles P. A., Hannikainen D. C., van Zyl L., 2005, ApJL, 634, L105

Eggleton P. P., Kiseleva-Eggleton L., 2001, ApJ, 562, 1012

Ford E. B., Kozinsky B., Rasio F. A., 2000, ApJ, 535, 385

Fregeau J. M., Cheung P., Portegies Zwart S. F., Rasio F. A., 2004, MNRAS, 352, 1

Fregeau J. M., Rasio F. A., 2006, ArXiv Astrophysics e-prints

Freire P. C. C., 2005, in Rasio F. A., Stairs I. H., eds, Binary Radio Pulsars Vol. 328 of Astronomical Society of the Pacific Conference Series, Eclipsing Binary Pulsars. pp 405–+

Fruchter A. S., Goss W. M., 1995, Journal of Astrophysics and Astronomy, 16, 245

Fryer C. L., 2004, ApJL, 601, L175

Giersz M., 2006, MNRAS, 371, 484

Gnedin O. Y., Zhao H., Pringle J. E., Fall S. M., Livio M., Meylan G., 2002, ApJL, 568, L23

Grindlay J., Portegies Zwart S., McMillan S., 2006, Nature Physics, 2, 116

Grindlay J. E., 1993, in Smith G. H., Brodie J. P., eds, The Globular Cluster-Galaxy Connection Vol. 48 of Astronomical Society of the Pacific Conference Series, X-Raying Stellar Remnants in Globular Clusters. pp 156–+

Grindlay J. E., Camilo F., Heinke C. O., Edmonds P. D., Cohn H., Lugger P., 2002, ApJ, 581, 470

Guerrero J., García-Berro E., Isern J., 2004, A&A, 413, 257

Gürkan M. A., Freitag M., Rasio F. A., 2004, ApJ, 604, 632

Gürkan M. A., Rasio F. A., 2003, in Piotto G., Meylan G., Djorgovski S. G., Riello M., eds, New Horizons in Globular Cluster Astronomy Vol. 296 of Astronomical Society of the Pacific Conference Series, The Radial Distribution of Millisecond Pulsars in 47 Tuc. pp 300–+

Harris W. E., 1996, AJ, 112, 1487, revision 2003

Heggie D. C., 1975, MNRAS, 173, 729

Heggie D. C., Hut P., McMillan S. L. W., 1996, ApJ, 467, 359

Heinke C. O., Grindlay J. E., Edmonds P. D., 2005, ApJ, 622, 556

Heinke C. O., Grindlay J. E., Edmonds P. D., Cohn H. N., Lugger P. M., Camilo F., Bogdanov S., Freire P. C., 2005, ApJ, 625, 796

Heinke C. O., Grindlay J. E., Lugger P. M., Cohn H. N., Edmonds P. D., Lloyd D. A., Cool A. M., 2003, ApJ, 598, 501

Heinke C. O., Wijnands R., Cohn H. N., Lugger P. M., Grindlay J. E., Pooley D., Lewin W. H. G., 2006, ApJ, 651, 1098

Hobbs G., Lorimer D. R., Lyne A. G., Kramer M., 2005, MNRAS, 360, 974

Holman M., Touma J., Tremaine S., 1997, Nature, 386, 254

Hurley J. R., Pols O. R., Tout C. A., 2000, MNRAS, 315, 543

Hut P., 2006, ArXiv Astrophysics e-prints

Innanen K. A., Zheng J. Q., Mikkola S., Valtonen M. J., 1997, AJ, 113, 1915

Israel G. L., Campana S., Dall'Osso S., Muno M. P., Cummings J., Perna R., Stella L., 2007, ArXiv Astrophysics e-prints

Ivanova N., 2006, ApJ, 636, 979

Ivanova N., Belczynski K., Fregeau J. M., Rasio F. A., 2005, MNRAS, 358, 572

Ivanova N., Belczynski K., Kalogera V., Rasio F. A., Taam R. E., 2003, ApJ, 592, 475

Ivanova N., Fregeau J. M., Rasio F. A., 2005, in Rasio F. A., Stairs I. H., eds, ASP Conf. Ser. 328: Binary Radio Pulsars Binary Evolution and Neutron Stars in Globular Clusters. pp 231–+

Ivanova N., Heinke C. O., Rasio F. A., Taam R. E., Belczynski K., Fregeau J., 2006, ArXiv Astrophysics e-prints

Ivanova N., Rasio F., 2004, in Revista Mexicana de Astronomia y Astrofisica Conference Series Compact Binaries in Globular Clusters. pp 67–70

Ivanova N., Rasio F. A., 2005, in Burderi L., Antonelli L. A., D'Antona F., di Salvo T., Israel G. L., Piersanti L., Tornambè A., Straniero O., eds, AIP Conf. Proc. 797: Interacting Binaries: Accretion, Evolution, and Outcomes Formation and evolution or compact binaries with an accreting white dwarf in globular clusters. pp 53–60

Ivanova N., Rasio F. A., Lombardi J. C., Dooley K. L., Proulx Z. F., 2005, ApJL, 621, L109

Ivanova N., Taam R. E., 2003, ApJ, 599, 516

Ivanova N., Taam R. E., 2004, ApJ, 601, 1058

Jacoby B. A., Cameron P. B., Jenet F. A., Anderson S. B., Murty R. N., Kulkarni S. R., 2006, ApJL, 644, L113

Jordán A., Côté P., Ferrarese L., Blakeslee J. P., Mei S., Merritt D., Milosavljević M., Peng E. W., Tonry J. L., West M. J., 2004, ApJ, 613, 279

Kawai Y., Saio H., Nomoto K., 1987, ApJ, 315, 229

King A. R., Pringle J. E., Wickramasinghe D. T., 2001, MNRAS, 320, L45

Kozai Y., 1962, AJ, 67, 591

Kroupa P., 2002, Science, 295, 82

Kundu A., Maccarone T. J., Zepf S. E., 2002, ApJL, 574, L5

Kundu A., Maccarone T. J., Zepf S. E., 2007, ArXiv Astrophysics e-prints

Kuranov A. G., Postnov K. A., 2006, Astronomy Letters, 32, 393

Levan A. J., Wynn G. A., Chapman R., Davies M. B., King A. R., Priddey R. S., Tanvir N. R., 2006, MNRAS, 368, L1

Lombardi J. C., Proulx Z. F., Dooley K. L., Theriault E. M., Ivanova N., Rasio F. A., 2006, ApJ accepted

Lyne A. G., Manchester R. N., D'Amico N., 1996, ApJL, 460, L41+

Mazeh T., Shaham J., 1979, A&A, 77, 145

Miller M. C., Hamilton D. P., 2002, ApJ, 576, 894

Miyaji S., Nomoto K., Yokoi K., Sugimoto D., 1980, PASJ, 32, 303

Nomoto K., 1984, ApJ, 277, 791

Nomoto K., 1987, ApJ, 322, 206

Origlia L., Rich R. M., 2004, AJ, 127, 3422

Ortolani S., Barbuy B., Bica E., Zoccali M., Renzini A., 2007, ArXiv e-prints, 705

Pfahl E., Rappaport S., Podsiadlowski P., 2002, ApJ, 573, 283

Podsiadlowski P., Langer N., Poelarends A. J. T., Rappaport S., Heger A., Pfahl E., 2004, ApJ, 612, 1044

Pols O. R., Schroder K.-P., Hurley J. R., Tout C. A., Eggleton P. P., 1998, MNRAS, 298, 525

Pooley D., Hut P., 2006, ApJL, 646, L143

Pooley D., Lewin W. H. G., Anderson S. F., et al. 2003, ApJL, 591, L131

Pryor C., Meylan G., 1993, in Djorgovski S. G., Meylan G., eds, ASP Conf. Ser. 50: Structure and Dynamics of Globular Clusters Velocity Dispersions for Galactic Globular Clusters. pp 357–+

Ransom S. M., Hessels J. W. T., Stairs I. H., Freire P. C. C., Camilo F., Kaspi V. M., Kaplan D. L., 2005, Science, 307, 892

Rappaport S., Verbunt F., Joss P. C., 1983, ApJ, 275, 713

Rasio F. A., Baumgardt H., Corongiu A., D'Antona F., Fabbiano G., Fregeau J. M., Gebhardt K., Heinke C. O., Hut P., Ivanova N., Maccarone T. J., Ransom S. M., Webb N. A., 2006, ArXiv Astrophysics e-prints

Rasio F. A., Pfahl E. D., Rappaport S., 2000, ApJL, 532, L47

Rosswog S., 2006, in Munster W., Kremer eds, NIC Symposium 206 Stellar Encounter with Black Holes. pp 39–46

Rutledge R. E., Bildsten L., Brown E. F., Pavlov G. G., Zavlin V. E., 2002, ApJ, 578, 405

Saio H., Nomoto K., 1985, A&A, 150, L21

Saio H., Nomoto K., 2004, ApJ, 615, 444

Scheck L., Kifonidis K., Janka H. ., Mueller E., 2006, ArXiv Astrophysics e-prints

Siess L., 2006, A&A, 448, 717

Sigurdsson S., Phinney E. S., 1995, ApJ Supp, 99, 609

Sivakoff G. R., Jordán A., Sarazin C. L., Blakeslee J. P., C{\ˆo}t{\' e} P., Ferrarese L., Juett A. M., Mei S., Peng E. W., 2006, ArXiv Astrophysics e-prints

Stairs I. H., Begin S., Ransom S., Freire P., Hessels J., Katz J., Kaspi V., Camilo F., 2006, in American Astronomical Society Meeting Abstracts New Pulsars in the Globular Cluster M28. pp 159.02–+

Tauris T. M., Takens R. J., 1998, A&A, 330, 1047

Thompson C., Duncan R. C., 1993, ApJ, 408, 194

Timmes F. X., Woosley S. E., 1992, ApJ, 396, 649

Timmes F. X., Woosley S. E., Taam R. E., 1994, ApJ, 420, 348

Timmes F. X., Woosley S. E., Weaver T. A., 1996, ApJ, 457, 834

van den Heuvel E. P. J., 1984, Journal of Astrophysics and Astronomy, 5, 209

van Kerkwijk M. H., Kaspi V. M., Klemola A. R., Kulkarni S. R., Lyne A. G., Van Buren D., 2000, ApJ, 529, 428

Verbunt F., Hut P., 1987, in Helfand D. J., Huang J.-H., eds, IAU Symp. 125: The Origin and Evolution of Neutron Stars The Globular Cluster Population of X-Ray Binaries. pp 187–+

Verbunt F., Lewin W. H. G., 2004, astro-ph/0404136

Webbink R. F., 1984, ApJ, 277, 355

Webbink R. F., 1985, in Goodman J., Hut P., eds, IAU Symp. 113: Dynamics of Star Clusters Structure parameters of galactic globular clusters. pp 541–577

Weinberg S., 1972, Gravitation and Cosmology: Principles and Applications of the General Theory of Relativity. ISBN 0-471-92567-5. Wiley-VCH , July 1972.

Wickramasinghe D. T., Ferrario L., 2005, MNRAS, 356, 1576

Wijnands R., Heinke C. O., Pooley D., Edmonds P. D., Lewin W. H. G., Grindlay J. E., Jonker P. G., Miller J. M., 2005, ApJ, 618, 883

Zepf S. E., Maccarone T. J., Kundu A., 2006, in AAS/High Energy Astrophysics Division Vol. 9 of AAS/High Energy Astrophysics Division, Testing Models of the Effects of Metallicity on LMXB Formation and Evolution. pp 01.63–+